





Do Salinity Variations Along the East Greenland Shelf Show Imprints of Increasing Meltwater Runoff?

Ilana Schiller-Weiss¹ , Torge Martin¹ , Johannes Karstensen¹ , and Arne Biastoch^{1,2} 

¹GEOMAR Helmholtz Centre for Ocean Research Kiel, Kiel, Germany, ²Christian-Albrechts-Universität Kiel, Kiel, Germany

Key Points:

- During 1993–2019, the East Greenland Coastal Current is freshest in 2010 and 2012 notably matching years of exceptional Greenland runoff
- Freshwater anomalies from sea-ice melt and Arctic export advected along east Greenland are of similar magnitudes as those linked to runoff
- Simulation of fresh coastal waters requires improved surface boundary conditions and/or models capable of representing mesoscale dynamics

Supporting Information:

Supporting Information may be found in the online version of this article.

Correspondence to:

I. Schiller-Weiss,
ischiller-weiss@geomar.de

Citation:

Schiller-Weiss, I., Martin, T., Karstensen, J., & Biastoch, A. (2023). Do salinity variations along the East Greenland shelf show imprints of increasing meltwater runoff? *Journal of Geophysical Research: Oceans*, 128, e2023JC019890. <https://doi.org/10.1029/2023JC019890>

Received 19 APR 2023

Accepted 20 SEP 2023

Abstract Accelerated melting of the Greenland Ice Sheet is considered a tipping element in the freshwater balance of the subpolar North Atlantic (SPNA). The East Greenland Current (EGC) and Coastal Current (EGCC) are the major conduits for transporting Arctic-sourced and Greenland glacial freshwater. Understanding freshwater changes in the EGC system and drivers thereof is crucial for connecting tipping elements in the SPNA. Using the eddy-rich model VIKING20X (1/20°) and Copernicus GLORYS12 (1/12°), we find that from 1993 to 2019 freshwater remains close to the shelf with interannual extremes in freshwater content (FWC) attributable to the imprint of Greenland melt only in years 2010 and 2012. Runoff increased significantly from 1995 to 2005 and Arctic freshwater export after 2005. Overall, regional wind patterns, sea ice melt and increasingly glacial ice and snow meltwater runoff along with the Arctic-sourced Polar Water set interannual FWC variations in the EGC system. We emphasize that these freshwater sources have different seasonal timing. South of 65°N sea ice melts year round and retreats to north of 65°N, where melt in summer prevails. Greenland runoff peaks in June–August with only some locations of year round discharge. Alongshore winds intensify in fall and winter where reduced onshore Ekman transport allows for freshwater to spread laterally in the EGC. We show that sea ice melt, runoff and wind can cause interannual variations of comparable magnitude. All of which makes attributing ocean freshening events to Greenland meltwater inflow at current magnitudes a major challenge.

Plain Language Summary The intensity of Greenland ice sheet melt has greatly accelerated over the past decades bringing more freshwater to the surrounding ocean. The additional freshwater has the potential to reach areas where deep waters are formed, which are an important part of the global ocean circulation. A lid of cool and low salinity water would weaken deep water formation and circulation affecting global heat redistribution. In this study we use a high-resolution model to investigate the effect of Greenland melt, sea ice export, and alongshore winds on freshwater content in the East Greenland Current and its coastal twin from Fram Strait to Cape Farewell. Two fresh extremes in 2010 and 2012 are attributable to local Greenland runoff maxima. We find that it takes 4–8 months for freshwater to propagate all along Greenland's east coast, with freshwater anomalies originating from the Arctic Ocean and additional input from sea ice melt along the journey often masking the Greenland runoff signal. Our results emphasize the need for ocean models and observations to resolve and record meltwater runoff, fjord and shelf processes, and boundary current dynamics to detect and attribute local freshening events.

1. Introduction

The East Greenland Current (EGC) provides a primary pathway of freshwater between the Arctic and North Atlantic (Haine et al., 2015). The freshening of the Arctic Ocean and the increase in ice-mass loss due to climate change on Greenland are additional sources of freshwater to the subpolar North Atlantic (SPNA) (Böning et al., 2016; Haine et al., 2015). Modulations in salinity can have far reaching impacts in the North Atlantic as changes affect the density stratification. This in turn may affect deep convection as additional freshwater input increases buoyancy, leading to a dampening of deep convection which in turn reduces aspects of the overturning circulation strength (Bakker et al., 2016; Böning et al., 2016; de Steur et al., 2016; Dickson et al., 1988; Tesdal et al., 2018; Zou et al., 2020).

While Greenland ice sheet melt has sharply accelerated during the recent decades, the contribution from melt alone is insufficient to explain the freshening trend in the SPNA (Friedman et al., 2017; Holliday et al., 2020) as there likely has not been sufficient freshwater input from Greenland to the regions that would directly affect deep convection and eventually the Atlantic Meridional Overturning Circulation (AMOC) strength (Böning

© 2023 The Authors.

This is an open access article under the terms of the [Creative Commons Attribution-NonCommercial License](https://creativecommons.org/licenses/by-nc/4.0/), which permits use, distribution and reproduction in any medium, provided the original work is properly cited and is not used for commercial purposes.

et al., 2016; Dukhovskoy et al., 2019; Jackson & Wood, 2018; Luo et al., 2016; Rahmstorf et al., 2015; Swingedouw et al., 2012). Recent high-resolution model comparisons show that the effect on meltwater redistribution and local response patterns is strongly dependent on eddy-resolving capabilities (Martin & Biastoch, 2023; Swingedouw et al., 2022). From the Greenland coastline to the open ocean, the main export pathway of liquid freshwater from Greenland melting sources and particularly Arctic export is manifested in the total freshwater content (FWC) flowing with the EGC south of Fram Strait (de Steur et al., 2018).

The freshwater pathways from the EGC to the deep convective sites in the Irminger and Labrador Sea are still not fully understood. Observational data shows that freshwater primarily flows along the boundary currents such as the EGC, the West Greenland Current, and following the Labrador Current (Bacon et al., 2002; Dickson et al., 2006; Dukhovskoy et al., 2015; Myers et al., 2009; Sutherland & Pickart, 2008). Cold and fresh waters originating from the EGC is found in the vertical structure of the West Greenland Current, where eddies form and shed along the West Greenland transporting heat and freshwater toward the interior Labrador Sea (Fischer et al., 2018; Rieck et al., 2019). South of Greenland at Cape Farewell, (Holliday et al., 2007) observed a retroflection which provides a direct pathway for freshwater to enter the interior of the gyre. Strong wintertime northeasterly wind and tip jet events can also export freshwater from East Greenland into the interior Irminger Sea (Duyck et al., 2022; Moore, 2012). As the EGC is a major conduit of freshwater from the Arctic and Greenland melt, it is of importance to unravel the complexities of the EGC system and better understand the fate of freshwater and its impact on the SPNA.

The EGC system has been observed to flow southward in two velocity cores (Le Bras et al., 2018), confirmed by moorings along the Overturning in the Subpolar North Atlantic Program (OSNAP, (Lozier et al., 2019)) East section, that extends from the Greenland shelf to Scotland through the central Irminger Sea (Le Bras et al., 2018; Lozier et al., 2019). The East Greenland Coastal Current (EGCC) is surface-intensified and carries cold and fresh water on the shelf (Le Bras et al., 2018). South of Denmark Strait, the EGCC is a well-known feature (Bacon et al., 2002; Foukal et al., 2020; Håvik et al., 2017; Sutherland & Pickart, 2008).

Just offshore is the shelfbreak branch of the EGC which separates fresh, cold shelf waters from warmer, saltier waters of the interior basin (Bacon et al., 2002; Håvik et al., 2017; Le Bras et al., 2018; Sutherland & Pickart, 2008). North of 71°N, Håvik et al. (2017) observed an offshore velocity core which they term the “outer EGC.” South of 64°N where the EGC and Irminger Current merge and flow at the shelfbreak, Le Bras et al. (2018) refer to that current branch as the slope current. In order to avoid confusion between these terms, slope current and outer EGC, we will refer to EGC flowing along the slope, beyond the shelfbreak, as the outer EGC.

Freshwater transport (FWT) along the EGC system has a strong seasonality, reaching a maximum during winter in concurrence with strong northerly, downwelling-favorable winds along the shelf (Foukal et al., 2020; Le Bras et al., 2018; Luo et al., 2016). Downwelling favorable winds induce onshore Ekman transport which constrains the low salinity water near the shelf, while upwelling is associated with offshore transport and eventually allow for freshwater to intrude into the interior basin (Castelao et al., 2019; Håvik & Våge, 2018; Luo et al., 2016; Oltmanns et al., 2018; Sutherland & Pickart, 2008).

In summer, winds weaken and are less downwelling-favorable, increasing the likelihood for intermittent offshore FWT (Håvik & Våge, 2018; Våge et al., 2018) which coincides with Greenland melt during summer. As the potential for extreme Greenland summer melt episodes may increase in the future, it is of interest to determine the role onshore and offshore transport plays on freshwater.

In this study we focus on the EGCC and outer EGC from Fram Strait (78.5°N) to Cape Farewell. We take cross sections along East Greenland and isolate the EGCC/outer EGC to investigate the FWC variability from a high-resolution model (1/20°) and reanalysis product (1/12°). We look at the effect of Ekman transport and analyze the evolution of freshwater in the East Greenland boundary current system, considering associated sources that is, Greenland and sea ice melt and Arctic export. We break down the overarching question of whether Greenland Ice Sheet melting and its recent increase (i.e., (Hanna et al., 2008; Rignot et al., 2011)) adds a significant amount of freshwater into the Greenland boundary current system into the following subtopics: the imprint of Greenland runoff and freshwater propagation along the East Greenland shelf, processes which drive salinity changes and FWT along the EGC system, and the significance of freshwater sources and temporal changes.

Section 2 describes the ocean model, reanalysis, and in situ observations, as well as the methods to compute FWC and EGCC/EGC variability. Section 3 starts with potential imprints of anomalous Greenland runoff in

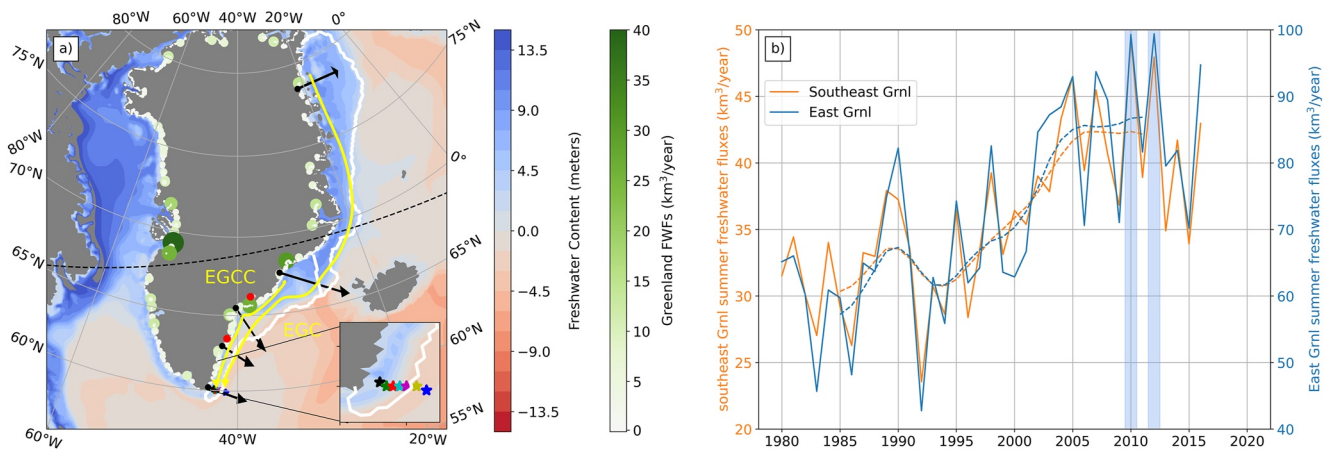


Figure 1. (a) Mean freshwater content for the years 1993–2019 computed from VIKING20X output based on a reference salinity of 34.8 psu. White to green dots encircling the Greenland coast show the integrated annual freshwater flux (FWF) estimates (Bamber et al., 2018) over the same period. The major current pathways of the East Greenland Current system are represented with yellow lines. Black arrows indicate cross sections discussed in the manuscript. The seven Overturning in the Subpolar North Atlantic Program mooring stations are marked as stars off of Cape Farewell, with an inset zooming into the Cape Farewell region. The red dots indicate the locations at Kangerlussuaq (68.63°N) and Helheim glaciers (66.35°N). The white contour shows the 1000 m isobath used to define the offshore boundary of the two regions of focus: the entire east Greenland shelf (59–80°N) and southeast Greenland shelf (59–69°N). The black dashed line indicates the extent of the regional nest, with the ocean grid refined to 1/20° south of the line. (b) Summer (June–August) FWFs along southeast Greenland (blue) and the entire east Greenland shelf (orange). The dashed blue and orange lines show the decadal running mean over the respective regions. The two extreme summers (2010 and 2012) are highlighted by the vertical blue thick lines.

the EGC system in southeast Greenland, the investigating the role of different freshening sources, such as Fram Strait export, propagation along the Greenland shelf, sea ice melt, runoff and wind regimes concluding with a composite analysis contrasting the different contributions on FWC. Lastly Section 4 considers the context and implications of freshwater variability along East Greenland.

2. Data and Methods

2.1. Description of Data Sets

2.1.1. Ocean Model

Freshwater variability along the East Greenland shelf is investigated using the ocean general circulation model VIKING20X (Biaostoch et al., 2021) an updated version of the original VIKING20 model configuration (Behrens, 2013; Böning et al., 2016). VIKING20X employs the NEMO3.6 ocean (Madec et al., 2016) and LIM2 sea-ice models (Fichefet & Morales Maqueda, 1997) on a tripolar Arakawa C grid. The model uses two-way nesting with Adaptive Grid Refinement in Fortran (AGRIF, (Debreu et al., 2008)) with a global host model at 1/4° (ORCA025) and regional horizontal grid refinement to 1/20° extending from the Nordic Seas to the southernmost tip of the African continent (34°S–70°N). The northern boundary of the nest is indicated by the black dashed line in Figure 1 where any latitudes south of the dashed line have a resolution of 1/20° and north is at 1/4° (see Biaostoch et al., 2021, their Figure 1). There are 46 depth levels increasing from 6 m thickness near the surface to 250 m in the deep ocean. The higher, eddy-rich resolution enables significant improvements in explicitly simulating mesoscale variability, which improves, for instance, Labrador Sea deep convection and AMOC variability (Biaostoch et al., 2021; Rühls et al., 2021).

The JRA55-do reanalysis is applied for atmospheric forcing, available at a 3-hourly temporal resolution on a 1/2° horizontal grid (Tsujino et al., 2018). JRA55-do version 1.4 also provides spatially and monthly varying meltwater runoff and iceberg discharge in terms of freshwater fluxes (FWFs) from Greenland based on (Bamber et al., 2018), elsewhere daily river runoff at 1/4° resolution is applied. As the FWF data does not extend beyond 2016, JRA55-do v1.4 repeats the FWF from Greenland of 2016 thereafter. In the VIKING20X simulations solid discharge is assumed liquid and applied as a combined field with river runoff. Runoff is assumed to have sea surface temperature, that is, any heat flux associated with solid discharge or liquid runoff is omitted. Sea surface restoring is also applied based on the World Ocean Atlas 2013 (Locarnini et al., 2013; Zweng et al., 2013).

climatology at a rate of 12.2 m/yr (timescale of 183 d for the 6 m thick surface layer). The restoring flux is not applied in an 80 km radius from Greenland to avoid a local, instant compensation of the enhanced runoff from ice-sheet melt. The coastal mask and the relatively weak salinity restoring facilitate a most realistic representation of Greenland-sourced freshwater in the SPNA while maintaining stability of the simulation.

We analyze monthly output of the VIKING20X-JRA-short run (Biaostoch et al., 2021) from January 1993 to December 2019, the overlap period with the GLORYS12 reanalysis (see Section 2.1.2). Figure 1a provides an overview of the general FWC in the model over this period. Runoff from the major glacier and fjord outlets is indicated by the white to green dots, the size signifying the magnitude of the cumulative FWF over the same period. Note, FWF is used synonymous with runoff throughout the study and includes the “liquified” discharge flux.

To illustrate the recent increase in runoff, its total over the southeastern shelf and entire east Greenland from summers (June–August) of 1980–2016 is shown in Figure 1b. We define the East Greenland shelf to be bounded offshore by the 1000 m isobath with a latitudinal extent from just north of Fram Strait (78.5°N) to Cape Farewell at 59°N (Figure 1a). The southeastern Greenland region is defined in agreement with (Sutherland & Pickart, 2008) and its FWF contributes ~50% to all runoff entering the ocean from East Greenland. In both regions the runoff steadily increased starting in 1995 up to 2005 with strong interannual variability thereafter and two maxima in 2010 and 2012.

2.1.2. Ocean Reanalysis

As Greenland meltwater enters the shelf and then interacts dynamically with the EGC system on local scales, high resolution observational data and coverage on the shelf would be needed but is sparse because of access limitations and shallow depth. High latitude—cold and ice covered—seas and, in particular, coastal and shelf regions are less well represented in remote sensing products (Garcia et al., 2017; Koehler et al., 2014; Olmedo et al., 2018), highlighting the importance of using high-resolution models to capture hydrodynamical instability processes in the SPNA for example, (Handmann, 2019). As a consequence, available ocean reanalysis products such as EN4 (Good et al., 2013) and ARMOR3D (Guinehut et al., 2012; Mulet et al., 2012) are also limited in their representation of the shelf seas around Greenland. They also lack in resolution for sampling the dynamical EGC system. Only the Copernicus Marine Environment Monitoring Service (CMEMS) global ocean physical reanalysis GLORYS12V1 (referred to as GLORYS12 throughout the manuscript) provided on a 1/12° grid is an assimilation model offering a holistic, near-eddy resolving estimate of global salinity, temperature, and velocities (Lellouche et al., 2021) and is used here for cross-validation with the eddy-resolving VIKING20X simulation. In addition both VIKING20X and GLORYS12 are validated with Overturning in the Subpolar North Atlantic Program moored data, see Text S2 in Supporting Information S1.

GLORYS12 contains 50 vertical levels at 1/12° horizontal resolution, covers the period 1993 to present, and assimilates in situ measurements and along-track satellite data via a Kalman Filter with a 3D multivariate modal decomposition of the background error into the model. The model component is based on NEMO driven at the surface by atmospheric conditions from ERA interim reanalysis output. In situ measurements include sea surface temperature data from NOAA, sea ice concentration from Ifremer/CERSAT, and the salinity and temperature vertical profiles are from CMEMS Coriolis Ocean Database for ReAnalysis (CORA) database which includes various in situ data (Argo profilers, moorings, underwater gliders, surface drifters, ship data) (Lellouche et al., 2021). In general, Argo floats from 2003 onward improve the reanalysis above 2000 m; however there are no Argo floats on the East Greenland shelf. Very few in situ measurements are included in the assimilation near the shelf, for example, OSNAP East mooring measurements are excluded. However when an in situ measurement is present, spatial and temporal correlation scales are used to define a sphere of influence around that grid point where the observation is present. A multivariate bias correction is added to enhance any observations that are within this bubble of influence, for example, if there is an available observation of sea level then the temperature and salinity increments can be deduced. It is only when observational coverage is completely insufficient or there is no direct constraint from the correlation scales based on proximity to an observation, then the ocean state is based on the numerical model (Dréville et al., 2021; Lellouche et al., 2021).

Some regional biases exist in GLORYS12 where the largest, cooler temperature bias lies in the 50–100 m layer in the North Atlantic. Sea surface salinity is generally fresher than when compared to the World Ocean Atlas (WOA) climatology, except in the Arctic where salinity tends to be higher than individual profiles suggest. While a slight

fresh bias exists, there are positive trends of sea surface salinity over most parts of the global ocean, with negative salinity trends found in the Arctic. Biases against all in situ observations decrease significantly with time as the density and number of observations increase (Lellouche et al., 2021).

GLORYS12's freshwater forcing differs from that applied to VIKING20X, particularly when replicating the additional freshwater input from ice sheet mass loss. In GLORYS12, there were two corrections made to the salinity field in order to avoid sea surface height drift from discrepancies in closing the water budget: first, the surface freshwater global budget was set to a seasonal cycle including 100 major rivers based on (Dai et al., 2008); second, a linear trend was imposed to the surface mass budget to replicate the freshwater sources from glaciers and ice sheet loss (Lellouche et al., 2021). For the period 1993–2001 the trend is 1.31 mm/yr and is increased to 2.2 mm/yr from 2002 onwards. These trends are implemented as a uniform surface FWF in ocean areas populated with observed icebergs (Lellouche et al., 2021), which for Greenland is based on the CERSAT Altiberg database for small and giant icebergs provided by Tournadre et al. (2015).

There intentions differ between the high-resolution ocean-only model VIKING20X and observation-assimilated reanalysis GLORYS12. VIKING20X is used to run a hindcast simulation (for sensitivity and process studies) based on ocean physics and constrained by surface fluxes providing a consistent though somewhat biased ocean state by construction. GLORYS12 aims to provide a holistic picture of the actual ocean state using a physical model but minimizing model biases by assimilating observations.

2.1.3. In Situ Observations

In order to examine the state of the northern boundary of our East Greenland delimited region (Figure 1a), VIKING20X and GLORYS12 are compared with 16 years of in situ salinity and velocity measurements at Fram Strait from September 2003 to August 2019 (de Steur et al., 2018; Karpouzoglou et al., 2022). The salinity and velocity measurements were collected from moorings at 78.5°N extending from 8° to 2°W by the Fram Strait Arctic Outflow Observatory (de Steur et al., 2018). The measurements are provided as monthly means on a 1/4° grid with the vertical resolution varying in depth (Karpouzoglou et al., 2022). While measurements at Fram Strait began in 1997, the mooring line was adjusted from 79°N to 78.5°N in 2002 where increased FWT was observed at the latter location. The coverage of the southward recirculating branch of the Return Atlantic Current also improved at the shifted mooring location (de Steur et al., 2018). Mooring measurements at OSNAP East were cross-validated with VIKING20X and GLORYS12 (Text S2 in Supporting Information S1).

2.2. Methods

We compute the FWC following (Haine et al., 2015; Marshall et al., 2017) using a reference salinity of 34.8 psu, which is consistent with previous studies and separates well between polar and Atlantic-origin waters (de Steur et al., 2016; Sutherland & Pickart, 2008). The FWC is presented for zonal cross-sections of specified latitude and horizontal maps, where for the latter it was integrated over the upper water column down to 200 m. For a single grid cell the FWC was computed as:

$$FWC = \iiint \frac{S_{ref} - S(t, z, y, x)}{S_{ref}} dz dy dx, \quad (1)$$

where S is the salinity and S_{ref} is the reference salinity. FWC represents the amount of zero-salinity water that would be required to reach the observed salinity, relative to a given reference salinity (Fuentes-Franco & Koenigk, 2019; Haine et al., 2015). A positive FWC implies that the salinity is fresher than the defined reference salinity. Given a cross section over a particular width and depth, the FWC is defined as the amount of freshwater present within that cross-sectional area.

We also investigate the FWT perpendicular to a cross section, in particular at Fram Strait to determine the amount of freshwater that is exported from the Arctic (discussed further in Section 3). Freshwater transport across a section is defined as:

$$FWT = \iint v_{\perp}(x, z) \cdot \frac{S(x, z) - S_{ref}}{S_{ref}} dz dx \quad (2)$$

where $v_{\perp}(x, z)$ corresponds to the velocity normal to the section specified by distance x and depth z . FWT differs from FWC in that it describes the volumetric flow rate at which freshwater is exported from upstream of the

section whereas FWC represents cumulative salinity variations below a given threshold. The FWT across a section further upstream can impact the FWC downstream.

Further, we compute Ekman transport components using the modeled wind stresses:

$$U_{ek} = \frac{\tau_y}{f\rho_0}, V_{ek} = \frac{-\tau_x}{f\rho_0}, \quad (3)$$

where $\tau_{x,y}$ is the wind stress provided by the ocean model, $\rho_0 = 1027 \text{ kg/m}^3$ is the density of sea water, and $f = 10^{-4} \text{ s}^{-1}$ is the Coriolis parameter.

The method to distinguish between the EGCC and the outer EGC velocity cores at the cross sections is described in Supporting Information S1 (see Text S1).

2.2.1. Composite Analysis

In Section 3.4, we perform a composite analysis to determine the impact of Greenland FWFs, alongshore wind stress, and sea ice production on the FWC using VIKING20X output. GLORYS12 has no wind stress or sea ice production output available. We refrained from computing the wind stress with ERA-interim reanalysis due to uncertainty about the exact bulk formulae used in GLORYS12.

We high pass filter Greenland FWFs, sea ice production, and FWC subtracting a 5-year Hamming-windowed running mean from the original time series to remove any decadal trends. This removes the signal of increasing Greenland FWFs from the early 1990s to mid-2000s (see Figure 1b), the recent eastern North Atlantic freshening (Holliday et al., 2020) and Great Salinity Anomaly of the 1990s (Belkin, 2004), and instead highlights seasonal to interannual variability. To illustrate the temporal variability of runoff, sea ice production, and winds stress along southeast Greenland, we take the gridcell area weighted mean of alongshore wind stress and spatially integrate the FWFs and sea ice production.

Then a cumulative sum of the monthly data is computed each year starting in January (FWFs and sea ice production) and June (wind stress). The different start date for wind stress is selected to allow comparability with Castela et al. (2019). The result is then used to obtain the members (individual years) for the FWC composites. Different months are chosen for each quantity to decide on the composite members: August for Greenland FWFs, May for sea ice production, and December for wind stress. These months are at or right after the peak of the cumulative sum of each quantity; only wind forcing continues to strengthen but we decided to focus on December for comparability with earlier studies.

For the respective months, each variable is grouped into categories of particularly anomalous years (15th and 85th percentile of the respective distribution). While these thresholds are too inclusive to consider the associated magnitudes as “extreme” (thresholds for cold spells/heat waves range from 10th/90th to 1st/99th percentiles (Frölicher et al., 2018; Hobday et al., 2018; Perkins-Kirkpatrick & Alexander, 2013)), some of the years included match such conditions. We determine the composite years for Greenland FWFs and sea ice production by subtracting: strong melt years minus reduced melt and weaker minus stronger alongshore wind stress. These composite years are used to compute the monthly FWC anomalies with implications discussed in Section 3.4.

3. Results

The following analysis aims at providing model-based evidence for a significant influence of glacial meltwater on the FWC of the EGC system in recent years. We begin with discussing variability of the FWC on the southeast Greenland shelf, where major outlet fjords are located. As internal variability proves large compared to such signal, we discuss the time varying export of freshwater from the Arctic Ocean through Fram Strait as an ultimate source of freshwater in the EGC, its southward propagation to Cape Farewell, the influence of local sea-ice melt, and the effect of the Ekman transport induced by differing wind stress magnitudes along the Greenland shelf. Lastly, a composite analysis looking at anomalous years of runoff, sea-ice melt and cumulative wind stress provides insight on magnitude and spatial distribution of these sources and factors driving low-salinity anomalies in the EGC system.

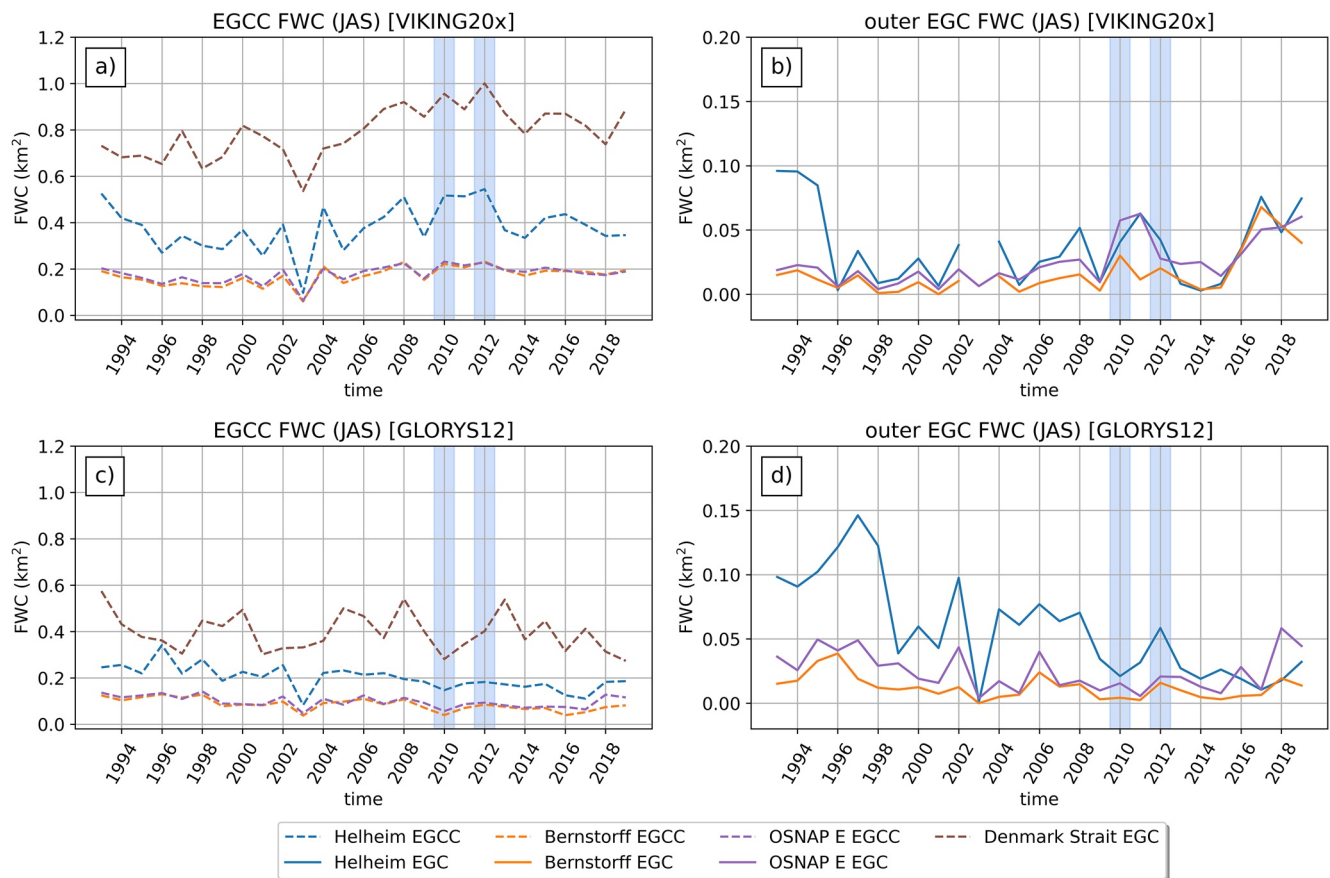


Figure 2. Time series of freshwater content (FWC) for VIKING20X and GLORYS12 per cross section. Panels (a) and (b) show the FWC from 1993 to 2019 for VIKING20X in the East Greenland Coastal Current (EGCC) and the outer East Greenland Current (EGC). The dashed lines indicate the EGCC, while the solid lines represent the outer EGC. Panels (c) and (d) show the same for GLORYS12. Note, y-axis ranges differ between left and right subfigures. The cross sections are south of Kangerlussuaq glacier at Denmark Strait (brown), south of Helheim glacier (blue), south of Bernstorff fjord (orange), and Overturning in the Subpolar North Atlantic Program East (purple). The two extreme runoff summers (2010 and 2012) are highlighted by the vertical blue thick lines.

3.1. Does Extreme Greenland Runoff Leave an Imprint on the East Greenland Shelf Hydrography?

3.1.1. Model Cross-Sections

Guided by the temporal evolution of the local runoff in southeast Greenland (Figure 1b), we select cross sections at Fram Strait (Arctic export gateway), Denmark Strait (south of Kangerlussuaq glacier), Helheim (south of Helheim glacier and at Sermilik trough), Bernstorff (south of Bernstorff Isfjord), and OSNAP East just off of Cape Farewell. These are all located within the nested area at $1/20^\circ$ resolution, only Fram Strait at 78.5° is outside of the nest.

The major current pathways of the EGCC and outer EGC are marked in yellow in Figure 1. Foukal et al. (2020) observed that the EGCC intensifies as it passes through Denmark Strait. Surface drifters also revealed the presence of the EGCC further north, flowing all the way from Fram Strait to Cape Farewell. However in both VIKING20X and GLORYS12, the EGCC was detectable only south of Denmark Strait, based on the criteria for two distinct, along stream velocity cores to be present at the shelf and beyond the shelfbreak (Text S1 in Supporting Information S1). Figure 1a only depicts the model state.

A seasonally varying mask based on salinity and southward-only velocity thresholds is applied (method described in Text S1 in Supporting Information S1). The annual summer (July–September) FWC variability in the EGCC and EGC per cross section are shown in Figure 2. Most of the freshwater in summer is contained within the EGCC, seen in both VIKING20X and GLORYS12 (Figures 2a and 2c). The total FWC decreases southward for various reasons: the narrower shelf leads to larger meridional current speeds facilitating a faster export of

freshwater and an increased exchange with saltier waters from the interior basin. The shelf boundary is indicated by the 1,000 m isobath nearing the coastline south of 65°N in Figure 1a.

The EGCC FWC in VIKING20X in Figure 2a shows an increasing annual FWC and interannual peaks resembling those of the Greenland runoff forcing applied in the model, notably at Denmark Strait and Helheim cross sections. In Figure 1b, there is a steady increase in the FWF over southeast Greenland starting in the 1990s until the early 2010s. The FWC increases up to 2012 in VIKING20X's EGCC south of Denmark Strait and Helheim glacier. Thereafter, Greenland FWFs appear to decline after 2012 and level off as does the annual FWC in the EGCC in the VIKING20X simulation.

There are interannual extremes in the FWC occurring in 2010 and 2012 in the EGCC in VIKING20X which coincide with the extremes in Greenland runoff imposed in the model (see Figures 1b and 2a). Interannually varying runoff included in the JRA55-do atmospheric forcing ends in 2016 and consequently the melt event reported for 2019 (Slater et al., 2021b) is not present in this VIKING20X simulation. For the 2010 extreme it was observed that an early onset of melting was triggered by anomalously warm near surface air temperatures which reduced surface albedo (Tedesco et al., 2011). The high air temperatures persisted throughout the summer resulting in a positive albedo feedback loop and caused additional melting in west Greenland (Tedesco et al., 2011). The summer of 2012 was a year marked by exceptional Greenland melt runoff due to negative North Atlantic Oscillation (NAO) conditions which advected warm southerly winds resulting in widespread surface melting (Hanna et al., 2014).

In contrast, GLORYS12 lacks a realistically varying runoff as a surface boundary condition and shows an overall decrease in FWC (Figure 2c). The EGCC is identifiable in GLORYS12 but is saltier near the shelf and surface, suggesting increased lateral mixing with the interior basin. Similar to VIKING20X, the northernmost cross sections are fresher than those downstream. Although subtle, there is a slight decrease in FWC from the early 1990s to mid-2010s for the sections south of Denmark Strait. This may be due to a consequence of the weaker constrain from actual in situ data for the assimilation process due to lack of observations close to the coast and at lower resolution.

The annual summer FWC in the outer EGC (Figures 2b and 2d) for both VIKING20X and GLORYS12 show a strong reduction in FWC presumably caused by mixing with saltier, warmer waters from the interior basin. In particular, the FWC decreases over time in the outer EGC at the Helheim cross section. There is a clear difference in interannual variability and patterns on a decadal time scale in GLORYS12. Compared to VIKING20X GLORYS12 only has a weak representation of the freshening after 2015 in the outer EGC. This increase in FWC in the outer EGC may be related to the recent eastern North Atlantic fresh anomaly (Holliday et al., 2020), as discussed by Rühls et al. (2021).

It is in particular the presence of sea ice and icebergs on the Greenland shelf that limits obtaining observational data in this region, including near surface waters (top 50 m). This holds true for mooring data from the OSNAP East array which provides no data above 50 m depth. As most of the freshwater is contained with the upper water column, near surface measurements remain critical (Karpouzoglou et al., 2022) and likely reflects in the skill of the reanalysis from GLORYS12. When excluding the top 50 m for the FWC in the EGCC at the Helheim section, the FWC decreases by 30% for VIKING20X. The reduction in FWC is even greater for GLORYS12, decreasing by 70%. The outer EGC for both models undergoes an even greater difference with a 70% reduction in FWC, highlighting the importance of the thin, near-surface layer above 50 m depth, as the freshest water is contained there.

The analysis of the cross sections along East Greenland reveals significant differences in FWC near the shelf between VIKING20X and GLORYS12. For VIKING20X, the EGCC FWC contains an increasing pattern with two interannual extremes which correspond to strong Greenland melt years of observed runoff. Meanwhile the FWC along the EGCC and outer EGC for GLORYS12 shows the FWC generally decreasing with time. The outer EGC shows a minimal freshwater imprint, demonstrating that most of the freshwater is constrained to the shelf and upper water layer.

3.2. How Does Freshwater Propagate Along the East Greenland Shelf?

3.2.1. Arctic Freshwater Export

A large source of freshwater in the EGC system is the export of polar water from the Arctic Ocean through Fram Strait. Arctic-sourced freshwater comes in two forms: liquid and solid sea ice flowing both on the shelf

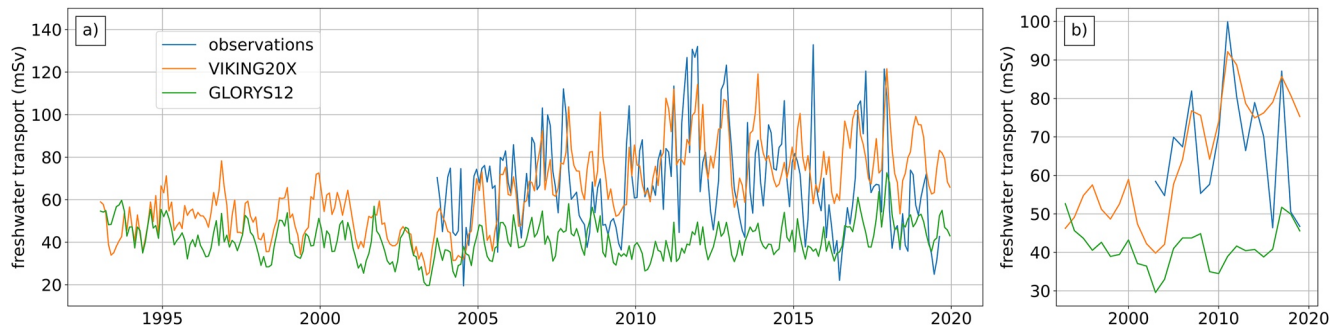


Figure 3. (a) The monthly Freshwater transport (FWT) from in situ observations at Fram Strait (78.5°) (blue), VIKING20X (orange), and GLORYS12 (green). (b) The annual mean FWT for the observations and models. Note the change in y limits on the vertical axis for the annual means.

and continental slope in the EGC (Holfort & Hansen, 2005). Sea ice export is primarily driven by alongshore, local winds (Smedsrud et al., 2008; Vinje, 2001). We investigate the FWT at Fram Strait as Arctic export sets the amount of low salinity polar water flowing south with the EGCC (Rudels et al., 2004). FWT differs from FWC in that it represents the volume of freshwater that is fluxed through the cross-sectional area, determined by both the flow velocity and salinity.

We compare the FWT estimates at Fram Strait between interpolated moored observations (Karpouzoglou et al., 2022), VIKING20X, and GLORYS12. The mooring line begins just off the shelfbreak from 8°W – 2°W at 78.5° , but for both models we extend the region from the shelf to 2°W , due to the availability of the shelf extent and that the freshest water is contained near the coastal branch of the EGC system (Bacon et al., 2014; Foukal et al., 2020; Le Bras et al., 2018).

The long term annual means for liquid FWT of polar water at Fram Strait is approximately 69 mSv given a reference salinity of 34.9 psu (Karpouzoglou et al., 2022). We recompute the FWT using the 34.8 psu and excluding any northward velocities, where the transport is calculated by Equation 2 to obtain a mean FWT of 68 mSv. Note that the Fram Strait cross section is outside the high-resolution nest in VIKING20X remaining on the global host model at $1/4^{\circ}$ resolution. Figure 3 shows the monthly and annual FWT for the observations, VIKING20X, and GLORYS12. The FWT is integrated from the shelf to 2°W (limit of the mooring array) for VIKING20X and GLORYS12, while the observations begin at the shelfbreak (Figure S3 in Supporting Information S1).

In Figure 3b, observational estimates from mooring data show an increased amount of FWT flowing across the section than VIKING20X and GLORYS12, particularly from 2003 to 2007. The long-term annual mean for the observations is 68 mSv, while VIKING20X and GLORYS12 have 62.7 and 41.4 mSv. GLORYS12 has lower FWT estimates due to freshwater reaching shallower depths in comparison to VIKING20X and the observations (Text S3 in Supporting Information S1). While closer to the observations in magnitude, the simulated temporal variability of VIKING20X resembles that of GLORYS12 more than that of the observations for the period 2003–2019 with correlation coefficients for monthly mean FWT of 0.64 to GLORYS12 and 0.45 to observations, while that for GLORYS to observations is only 0.27. The FWT estimates depend not only on salinity and velocity but also on the respective grid resolution. Freshwater does not extend as deep in the water column where the vertical grid cell sizes coarsen with increasing depth. Large grid cells may carry significant amounts of freshwater even when exceeding the constant threshold salinity only marginally; using partial grid cell volumes is not considered here.

On the other hand, the FWT for VIKING20X is comparable with the observations when the section includes the shelf (coastline to 2°W). There are deviations in interannual variability, particularly in Figure 3a, but the magnitudes appear consistent with observations. When the shelf is included, the FWT increases for VIKING20X suggesting that freshwater along Fram Strait remains near the shelf but freshwater offshore reach increased depths than GLORYS12.

Both models show an increase in the annual FWT from 2003, particularly in VIKING20X, which is not as evident in the observations as they begin in 2003 (Figure 3b). Although both models slightly underestimate the mean FWT at Fram Strait, in particular GLORYS12, there are differing biases in the models. VIKING20X has lower southward current speeds just off the shelfbreak at Fram Strait (Figure S3 in Supporting Information S1) but

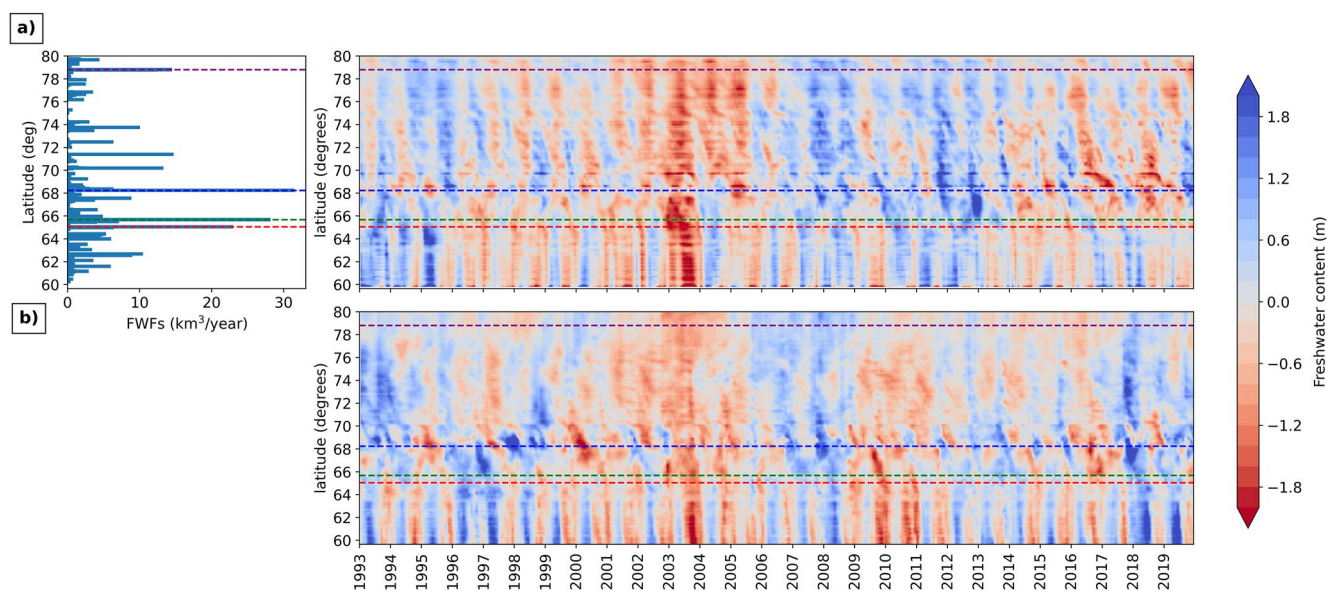


Figure 4. (a) The lefthand panel shows the annually integrated freshwater fluxes averaged over the period 1993–2016 from Greenland liquid and solid ice discharge (Bamber et al., 2018) per latitude. The dashed lines in purple, blue, green, and red indicate the top four largest runoff locations. The righthand top panel shows the evolution in freshwater content (FWC) anomalies over the reference period 1993–2019 per latitude for VIKING20X. (b) The FWC anomalies for GLORYS12.

comparable salinities to the observations across the section. Freshwater is transported downstream via Fram Strait closer onshore rather than offshore beyond the shelfbreak. Due to observational measurements lacking onshore, it is unclear if observations would result in an increased FWT provided on-shelf measurements were available however it would be of interest to see how magnitudes may vary if the entire shelf were included.

These discrepancies between the models and observations, particularly the reanalysis, highlight the need of obtaining a realistic representation of Fram Strait export, especially as this sets the amount of polar water flowing south with the EGCC (Rudels et al., 2004). The remaining analysis focuses on the origin and propagation of fresh anomalies and thus holds despite the described FWT biases at Fram Strait.

3.2.2. Downstream Freshwater Propagation From Fram Strait to Cape Farewell

As freshwater exported from the Arctic via Fram Strait plays a significant role in determining the initial low salinity near surface water of the EGC system, we investigate how freshwater propagates along the shelf from Fram Strait to Cape Farewell. Figure 4 shows Hovmoeller diagrams of the zonally integrated FWC on the east Greenland shelf for VIKING20X and GLORYS12. Given that Greenland FWFs enter through the surface and along the coastline, we determine the changes in FWC along the shelf computed from Equation 1 and integrated over the top 200 m. The mean FWC climatology over the EGC region (59–80°N) is calculated based on the reference period 1993–2019 and then the FWC anomalies are linearly detrended. The detrended FWC is used to focus on the salinity variations that arise from local melt and upstream freshwater sources on an interannual basis rather than any long-term evolution in Greenland runoff or Arctic export as discussed above (Figures 1b and 3b). Since the zonal extent of the 1000 m isobath varies in distance per latitude, the anomalies are standardized by dividing the total horizontal grid cell area per latitude, which reduces the overestimation of the FWC from changes in shelf width.

The righthand top panel of Figure 4a and the lower panel b show the monthly FWC anomalies for VIKING20X and GLORYS12, where positive FWC signifies fresher water than the climatology. There is strong interannual variability in VIKING20X and GLORYS12 with a period of greater salinities from 2003 to 2006. Since FWC was detrended, these do not originate from the long-term increase of Fram Strait FWT. Other differences between the models are in 2010 and 2012 when exceptional Greenland runoff occurred during those summers but the positive anomalies in FWC are not seen in GLORYS12.

In Figure 4a, the dashed lines indicate major runoff locations, displayed by the bar diagram of the land-sourced FWF (Bamber et al., 2018) per $\approx 0.2^\circ$ latitude in 4a. The monthly FWFs are accumulated per year and then averaged

over 1993–2016. There is a maximum of FWF from Greenland at $\approx 68^\circ\text{N}$ at Kangerlussuaq glacier; one of the largest glaciers along East Greenland. The next largest freshwater input comes from Helheim glacier ($\approx 66^\circ\text{N}$) and at 79°N where the 79°N glacier and Zachariae Isstroem glacier is located (Rignot & Mouginot, 2012). In GLORYS12, coastal runoff is represented by a spatially varying climatological FWF in combination with an additional, uniformly distributed FWF in regions of observed iceberg occurrence.

FWC anomalies propagate south but considerable local variability imprints on this signal, where the anomalies are generally larger in VIKING20X than in GLORYS12. The advective time scale from Fram Strait to Cape Farewell ranges between 4 and 8 months. Thus freshwater anomalies leaving the Arctic Ocean in mid-winter to spring can potentially interfere with and mask runoff anomalies in southeast Greenland, which peak in summer (July–August). Local offshore advection and mixing with saltier interior waters in the Nordic and Irminger seas contribute to the erosion of the anomaly along the way. The maximum in Greenland meltwater input occurs at the Kangerlussuaq glacier (68°N), just north of Denmark Strait. (Foukal et al., 2020) observed that freshwater flowing southward along the EGC tended to converge at Denmark Strait where downwelling-favorable winds drive onshore flow due to widening of the shelf north of Denmark Strait. This suggests that any meltwater output from the Kangerlussuaq glacier likely mixes with the initial low-salinity polar waters propagating southward from Fram Strait and would explain why there is not a strong positive FWC anomaly south of 68°N (Figures 4a and 4b).

Recirculation occurs at the deeper Kangerlussuaq trough at $\approx 67^\circ\text{N}$ where studies show that a net input of freshwater splits into the EGCC south of Denmark Strait with a return flow out of the trough (Foukal et al., 2020; Sutherland & Pickart, 2008). Arctic freshwater export and recirculation at the trough just south of the Kangerlussuaq glacier both contribute to FWC variability but likely obscure any additional signal from Greenland runoff.

After recirculation at the trough and freshwater convergence along the shelf due to strongly downwelling-favorable winds, meridional current speeds increase south of 65°N , reaching values up to 0.4 m/s in both models (Figure S1 in Supporting Information S1), which occurs where the 1,000 m isobath and shelfbreak steadily narrows. Given the high current velocities and the reduced distance freshwater travels, advection of freshwater from 65°N to 59°N happens within 1 month and hence the propagation of freshwater anomalies is not resolved by the monthly mean output of the models used here. This explains why in the Figures 4a and 4b Hovmoellers there are these vertical, instantaneous-like positive and negative FWC anomalies, implying a divergence of freshwater south of 64°N .

3.3. What Are the Processes Driving Salinity Variations and Freshwater Transport in the EGC?

3.3.1. Sea Ice Melt and Greenland Runoff

Apart from polar water and Greenland runoff, a significant freshening source is sea ice melting along the east Greenland shelf. We analyze the sea ice production output from VIKING20X (local freezing, when >0 , and melting rates, <0), a quantity not provided for GLORYS12, which includes sea ice thickness as a variable but not thermodynamic thickness change, that is, melt or freezing. A provisional reconstruction of such an ice production field based on month-to-month sea ice thickness changes is prone to failure because sea ice thickness change is dominated by advection in this region. Further analysis concentrates on VIKING20X output.

Figure 5a shows the seasonal cycle of sea ice production (blue colors imply meltwater input) per zonal section (meridional resolution of 10–20 km, ORCA025 grid) from VIKING20X. Sea ice production is zonally integrated over the east Greenland shelf within the 1,000 m isobath. For comparison, the seasonal cycle of runoff along east Greenland is shown per coastline gridpoint (Figure 5b). There is primarily sea ice formation throughout winter and early spring from 67 to 80°N . Sea ice melt occurs from summer to late fall peaking in June (67 – 70°N) and July (north of $\sim 71^\circ\text{N}$). North of $\sim 71^\circ\text{N}$ runoff begins to increase in late May, reaching a maximum in June/July then reduces in September. South of 70°N , there are some latitudes which have a positive Greenland FWF year-round (Figure 5b). The wintertime runoff is attributed to outlet glacier calving where solid ice discharge can enter the open ocean (Bamber et al., 2018) but have relatively lower magnitudes compared to summer runoff. Freshwater from sea ice melt coincides with the runoff peak but typically exceeds the latter, suggesting that additional freshwater from summertime sea ice melt further north propagating downstream can mask the local runoff signal.

Further south, from 65 to 67°N , sea ice melting occurs from late fall (November) to early summer (June). As there is no sea ice present in summer and early fall, most of the ice melting in this region originates further north and is

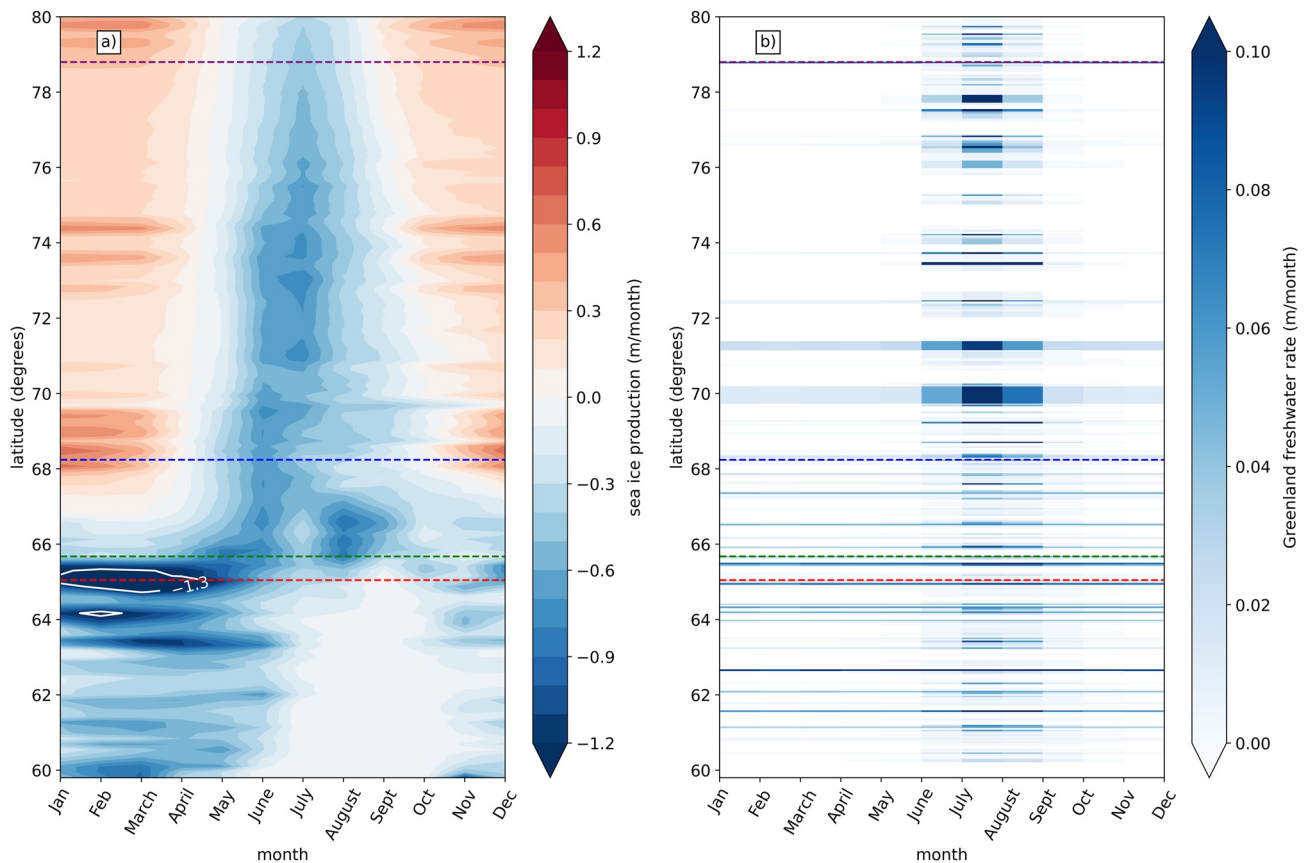


Figure 5. (a) Hovmöller plot showing the climatology of sea ice production (m/month) from VIKING20X over the reference period 1993–2019. Positive values indicate sea ice growth, while negative values signify melting. (b) Mean seasonal cycles of Greenland freshwater flux (FWF) (m/month) from Bamber et al. (2018) averaged over 1993–2019 per latitude band. The zonally integrated FWFs (km^3/month) are divided by the ocean model's grid cell area to convert to m/month for comparison with sea ice production depicted in panel (a). The white to blue colors indicate increasing FWFs per latitude (15° resolution). The dashed colored lines indicate the major Greenland runoff sources (see Figure 4a) showing the mean annual FWFs integrated over 1993–2016.

imported by the southward flow with only little formed and melted locally. This timing does not overlap with the runoff seasonal cycle featuring a marked summer peak. The melting of sea ice south from Cape Farewell (59°N) to Denmark Strait (66°N) during the late winter and early spring including the region of enhanced southward current speeds on the narrower shelf explains the persistent positive and negative freshwater volume anomalies that occur during early winter/spring in Figure 4.

South of Denmark Strait, we find that there has been a reduction in sea ice meltwater flux in the last 13 years with a linear trend of $-40.48 \text{ km}^3/\text{year}$ for the period 2006–2019. Interannual variability has strongly reduced from 217.6 km^3 (1993–2005) to 73.5 km^3 (2006–2019), likely from a reduction in the amount of sea ice available to melt. In VIKING20X sea ice export through Fram Strait declined from 1993 to 2019 by $11.86 \text{ km}^3/\text{yr}$ with a stronger trend of $42 \text{ km}^3/\text{yr}$ over the last 13 years, which matches recent observational estimates (Spreen et al., 2020; Wang et al., 2021).

Sea ice melt remains a significant source of freshwater entering the ocean locally but also being advected along the EGC. Freshwater from Greenland, Arctic export through Fram Strait, and sea ice melt on the Greenland shelf all contribute as freshwater sources to the EGC and EGCC systems, which carries the anomalies into the SPNA. Disentangling the individual signals remains a challenge, but the sources provide insight into how freshwater is transported and seasonally changes along the East Greenland shelf.

3.3.2. Effect of Wind Stress on Volume and Freshwater Transport

Alongshore winds play a large role on modulating cross-shelf transport of freshwater (Luo et al., 2016). The shallower EGCC in particular is observed to be both wind and buoyancy driven (Sutherland & Pickart, 2008).

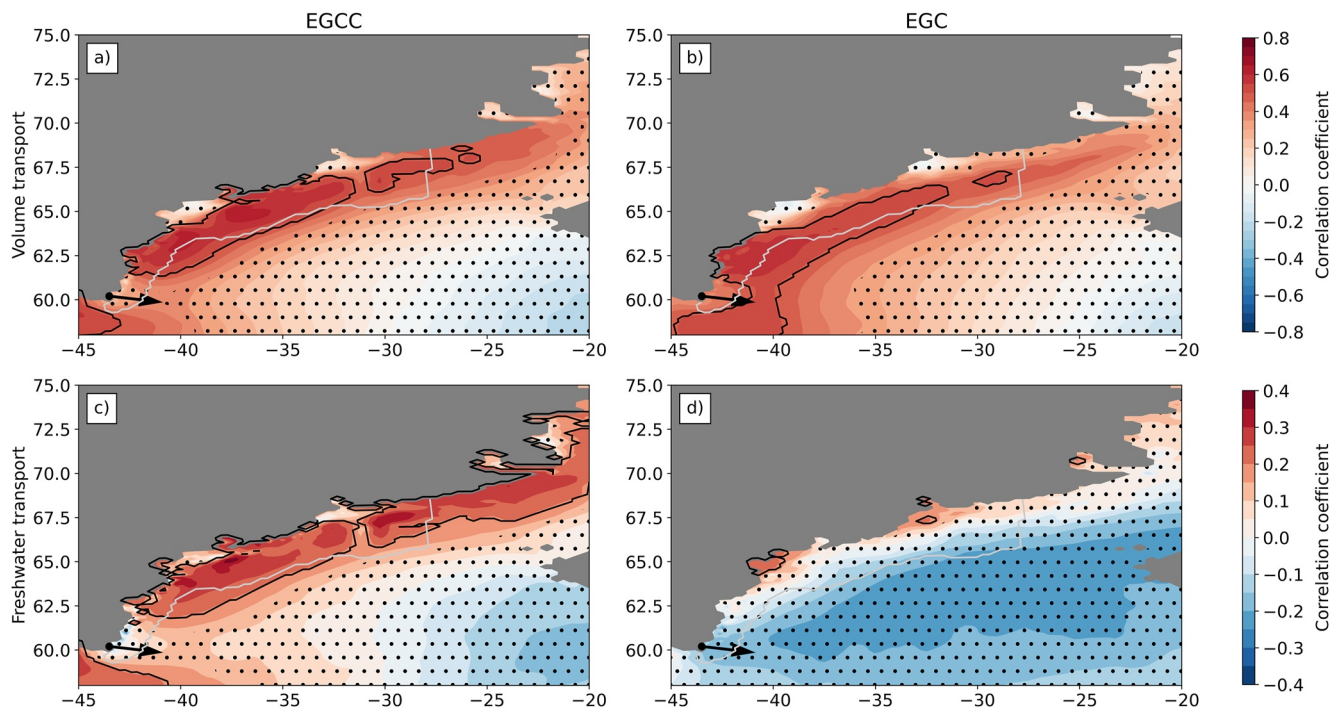


Figure 6. The following correlations are between the alongshore wind stress and the volume and Freshwater transport (FWT) at the Overturning in the Subpolar North Atlantic Program (OSNAP) East mooring line indicated by the black arrow. (a) Correlation between East Greenland Coastal Current (EGCC) volume transport from VIKING20X at OSNAP East mooring line location and alongshore wind stress. (b) correlation between alongshore wind stress and outer East Greenland Current (EGC) volume transport. For panels (a) and (b), the black contour shows coefficients greater than 0.5. (c) correlation between EGCC FWT with the wind stress. Note the change in colorbar limits. The black contour shows coefficients greater than 0.2. (d) Correlation between outer EGC FWT and alongshore wind stress. The gray contour indicates the southeast Greenland partition. Black dots indicate areas that are not significant.

We investigate the role of alongshore wind stress as being a driver of the EGCC and outer EGC transport variability in VIKING20X, as hypothesized by Le Bras et al. (2018). We focus on VIKING20X since surface wind stress is not provided for GLORYS12. GLORYS12 is forced with ERA-interim reanalysis wind speeds, but without detailed information on the bulk formulae used in GLORYS12 wind stress estimates would be associated with large uncertainty. Thus we only use VIKING20X output.

The OSNAP East EGCC and outer EGC monthly volume transport correlation is evaluated with the alongshore wind stress from 1993 to 2019 following similar analysis by Le Bras et al. (2018). We also evaluate the correlation of the FWT with the wind stress to investigate the effect of alongshore winds on salinity along the shelf. The correlation between the monthly alongshore wind stress and volume/FWT is computed at zero lag expecting no lag greater than 1 month between transport and wind forcing. We apply the method described in Section 2 to isolate the EGCC from the outer EGC at the location of OSNAP East. The correlations are evaluated at zero lag, where a one-tailed student t -test is used to determine the 99% confidence interval.

Figures 6a and 6b show the correlations between volume transport and alongshore wind stress for the EGCC and EGC. The correlation patterns agree well with those presented by Le Bras et al. (2018), (their Figure 10). The volume transport of the outer EGC shows further offshore correlations south of 65°N extending south of Cape Farewell. Upstream reaching positive correlations are explained by coherent high-speed northeasterly surface winds, which are maintained along the extent of the southeast Greenland coast (Moore, 2014). Le Bras et al. (2018) also noted that upstream wind stress may be transmitted southward by coastally trapped waves. The positive correlations between volume transport and alongshore winds show consistency with the mechanism that northerly alongshore winds result in primarily downwelling, where strong onshore Ekman transport steepens isopycnals, and southward flowing current velocities accelerate (Bacon et al., 2014; Harden et al., 2014; Le Bras et al., 2018; Sutherland & Pickart, 2008).

In VIKING20X, we find a larger spatial extent and higher positive correlations ($r \geq 0.5$) for the EGCC than reported by Le Bras et al. (2018). The correlation pattern of the EGCC presented here appears more similar to

that of the outer EGC in Le Bras et al. (2018), (their Figure 10). The EGCC's volume transport at OSNAP East is highly correlated with the alongshore wind stress further upstream and over the entire east Greenland shelf up to about 70°N. Interestingly, the correlation is not statistically significant directly at the mooring line. (Le Bras et al., 2018) noted that the mooring array may underestimate the EGCC volume transport, since the near-shelf velocity core is not consistently located below the CF1 mooring. There is only one CTD station located onshore, while in VIKING20X the entire shelf area is relatively well represented. On the other hand, VIKING20X may under-represent local, coastal processes, which could explain comparatively high and far upstream correlations with the wind stress.

To examine the wind's impact on freshwater anomalies, we present corresponding correlation maps with the FWT at OSNAP East in Figures 6c and 6d. Note that FWT contains volume transport and salinity anomalies (Equation 2). For the EGCC we find a similar correlation pattern but about 50% lower than for volume transport. Positive, significant correlation values extend just north of the OSNAP East cross section to north of Denmark Strait, indicating that alongshore winds strengthen the connectivity on the shelf. Stronger alongshore winds cause stronger onshore Ekman transport leading to a narrowing and acceleration of the EGCC. In consequence, freshwater is flushed faster downstream. There are positive correlations that reach south of 65° where the shelf is much narrower which is associated with further acceleration of the current. This is also evident in Figure 4 where the advective time scale for freshwater anomalies to travel downstream reduces to less than 1 month in both VIKING20X and GLORYS12 south of 65°N.

In contrast, FWT in the outer EGC is not significantly correlated with the wind stress. We find a rapid decrease from sparse positively correlated locations at the coast to widely negative ones in the interior Irminger Sea. Since FWT is a combination of volume transport and salinity anomalies, we conclude that FWT in the EGCC is partly wind- and partly salinity-driven whereas in the outer EGC it is mostly a function of salinity variations originating from mixing with either the fresher EGCC or the saltier Irminger current water adjacent to the outer EGC. FWC is larger on the shelf and increases toward the coast in both VIKING20X and GLORYS12 (see Figure 2) making the EGCC a significant freshwater conduit in southeast Greenland with alongshore winds influencing freshwater anomalies and their propagation around Cape Farewell.

3.4. What Is the Relative Importance of Freshwater Sources and Is It Changing Over Time?

Given the various freshwater sources along East Greenland, we will determine their relative impact on interannual variations in FWC in the EGC system. Please note that the following analysis focuses on VIKING20X, as neither wind stress nor sea ice production are available from GLORYS12. A composite analysis is done based on the cumulative Greenland runoff fluxes and sea ice production accumulated over the seasonal cycle (January–December) with alongshore wind stress accumulated from June–December (Castelao et al., 2019) (method described in Section 2).

We focus the composite analysis on southeast Greenland due to the immediate impact of additional freshwater input into the Irminger (Duyck et al., 2022; Holliday et al., 2007) and Labrador seas (Castelao et al., 2019; Gillard et al., 2016). This is justified by coherent large-scale atmospheric conditions, a short advective time scale and similar sea ice conditions (see sections above). The composite member years to determine the years of strong/weak meltwater from Greenland FWFs and sea ice melt alike are selected based the respective month in which the seasonal-based increase in freshwater input concludes that is, August for Greenland FWFs and May for sea ice production along southeast Greenland. The alongshore winds composite years are determined from December, as alongshore winds strengthen in winter and often drive near-surface FWT variability (Duyck et al., 2022; Sutherland & Pickart, 2008). The cumulative integral over the seasonal cycle for Greenland FWFs, sea ice production, and alongshore wind stress over southeast Greenland is shown in Figures 7a, 7c, and 7e. Resulting differences in FWC based on the composite analysis is presented in Figures 7b, 7d, and 7f. Additional information on a potential influence on stratification as preconditioning to deep convection later in January is provided in Text S4 in Supporting Information S1.

The cumulative time series from January to December for Greenland runoff shows strong seasonality with most runoff occurring from June to August indicated by the steeper, positive slope between those months (Figure 7a). Both the following winters after summers with exceptionally strong melt, 2010 and 2012, are included in the anomalously high runoff years. Notably, in southeast Greenland, the runoff in the summer of 2010 was greater than in 2012 (Figure 1b).

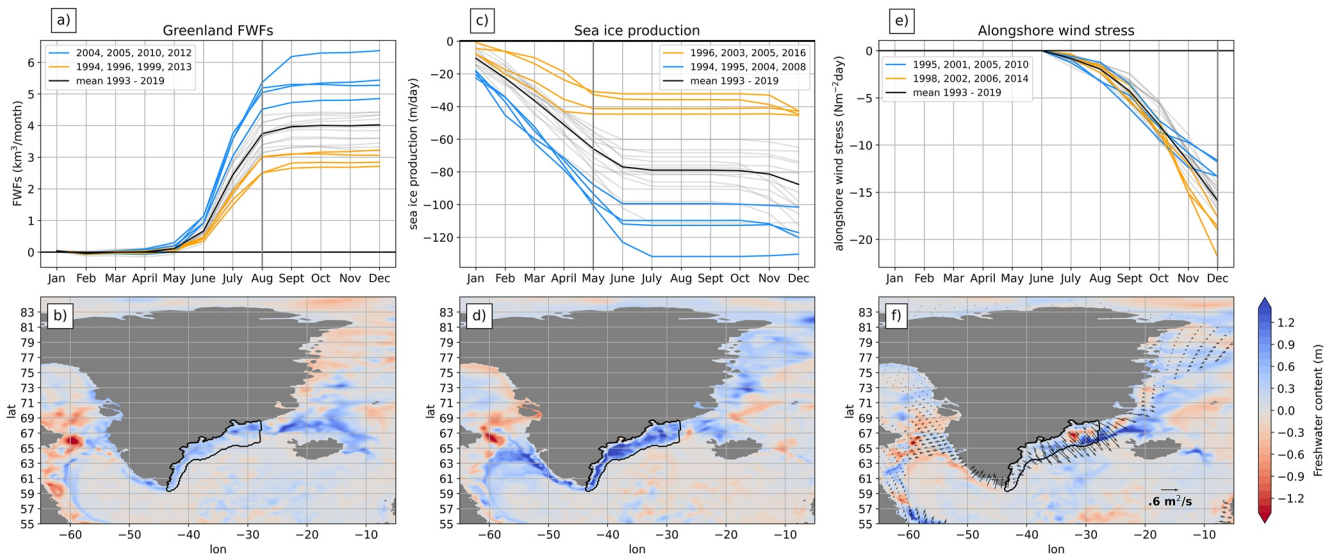


Figure 7. Panels (a), (c), and (e) show the cumulative Greenland melt, sea ice, and alongshore winds given the seasonal cycle starting over January/June–December. The gray line indicates the respective month which the composite to determine the freshwater content (FWC) anomalies are based on. The extreme years determined by a 15th percentile threshold are highlighted in yellow and blue. Panels (b), (d), and (f) show differences in FWC based on a composite analysis of Greenland freshwater flux and sea ice production (negative for melt) in August and for alongshore wind stress in December. Composite differences are computed by subtracting low runoff/melt years (orange lines in panels (a), (c)) from years with high rates (blue lines); for the wind stress based composite the mean of strong wind stress years (orange lines) is subtracted from weaker years (blue lines). The black contour shows the southeast Greenland partition. In panel (f) black vectors depict Ekman transport anomalies of December.

The spatial pattern of FWC composite differences (Figure 7b) shows enhanced FWC around the southeast Greenland shelf for strong runoff years compared to low years. There are patches of higher FWC anomalies particularly around Denmark Strait from 65 to 69°N, where the Kangerlussuaq glacier is located and where the EGC system is observed to converge at Denmark Strait and recirculation occurs at Kangerlussuaq trough. The composite difference reveals that this fresh anomaly is carried around Cape Farewell by the EGCC and outer EGC. The West Greenland Current, subsequent boundary current outlining the subpolar gyre, and further north along the shelf by Baffin Bay appear fresher in August just after the summertime peak in Greenland runoff. Years of increased freshwater release from the Greenland coastline show enhanced, positive FWC anomalies localized near the shelf and boundary current along southeast and West Greenland.

Figures 7c and 7d show the monthly cumulative sea ice production and the associated May FWC composite difference. In southeast Greenland region, sea ice melt occurs predominantly in winter and subsides in May (Figure 5a). Therefore, we find cumulative sea ice melt growing (steeper, negative slope) from November (strong melt years, blue lines in Figure 7c) and January (weak melt, orange lines) over winter. Interestingly, while both summers of 2010 and 2012 resulted in anomalous runoff, neither 2010 or 2012 is included in the composite years for sea ice production. We conclude there is no coherence between runoff and sea ice production. Instead, local sea ice melt is dominated by ice being advected into the southeast Greenland region.

For May we find a positive FWC anomaly from Cape Farewell up to Fram Strait for years of strong sea ice melt in southeast Greenland, suggesting that this is driven by a large-scale coherent forcing. There is a patch of positive anomalies by Denmark Strait, and south of 65°N where there are higher FWC anomalies along the boundary current which then follow along the west Greenland current and intrudes the northern Labrador sea. Sea ice melt results in increased FWC along the east and southwest Greenland shelf, reiterating that sea ice melting and formation plays a significant role in setting the FWC along the East Greenland shelf (de Steur et al., 2015). In contrast to the runoff composite, the positive, blue FWC anomaly on the southwest Greenland shelf is enhanced and connects to a fresh anomaly in the northern Labrador Sea, which otherwise is characterized by slightly reduced but comparable FWC anomaly magnitude.

We focus on the immediate impact on local FWC rather than freshwater having propagated from further upstream. It takes about 1 month for freshwater to be advected southward from 65°N but 4–8 months for freshwater to

propagate from Fram Strait to Cape Farewell (Figure 4). From the fast advection within a single month around Cape Farewell, southeast Greenland runoff anomalies will show as FWC anomalies on the southwestern shelf indicative of the known, strong influence of east Greenland runoff on the Labrador Sea. Similar for the wind, we look at the cumulative effect on FWC right at the end of its strengthening season in fall. Wind plays a dominant role in driving much of the near-surface freshwater on and offshore (Håvik & Våge, 2018).

Cumulative wind stress grows linearly from September onwards and hence contributes to FWC anomalies in December (Figure 7e). Negative alongshore wind stress values indicate primarily downwelling favorable winds (onshore Ekman transport), while values close to zero or positive indicate the potential for upwelling-favorable winds (offshore or weaker onshore transport). The December FWC anomaly is computed by subtracting the stronger alongshore winds from weaker northerly winds yielding anomalous offshore Ekman transport.

The December FWC and Ekman transport anomalies are shown in Figure 7f. We find a fresher EGC system particularly south of 65°N. Close to the shelfbreak, the FWC anomaly difference becomes minimal; over the interior Irminger and Labrador Sea it is weakly positive and negative. As indicated by the arrows, the associated Ekman transport anomaly points offshore, showing a weakening of the predominant onshore Ekman transport. This slackening of the wind forcing allows the fresh polar waters of the EGCC to expand over the shelf, and occasionally offshore across the shelf break. The composite shows that reduced onshore Ekman transport relaxes the EGCC and extends the width along which freshwater travels southward along the current. Meanwhile, strong onshore transport results in a steepening of isopycnals close to the shelf, restricting the freshwater and narrowing the boundary current, but allows for saline and warmer water from the interior basin to intrude on the outer EGC due to the strong winds pushing the water toward the shelf. Interestingly, we find 2005 and 2010 among the years with anomalously weak cumulative wind stress (favoring fresh conditions on the shelf), years that are also characterized by anomalously large runoff (cf. Figure 7a), which however occurred in summer prior to the wind stress anomaly. Here, we can only speculate that climate modes, such as the NAO, occasionally provide a link between these two factors in the EGCC freshening.

The Ekman transport anomalies show coherent behavior south of 71°N, which relates to the overlying large-scale atmospheric conditions but points at a different regime dominating farther north in the Greenland Sea. Here, the shelf is wider and eddy-driven mechanisms have been observed to dominate transport changes rather than the local wind stress, as westward transport of Atlantic water from the West Spitsbergen Current merges with the EGC via topographically steered eddies (Gascard et al., 1995; Richter et al., 2018). Approaching Cape Farewell, south of 63°N, Ekman transport anomalies tend to reduce. More importantly, on the southwestern side of Greenland the anomaly is rather onshore suggesting that in winters, in which the southeast Greenland shelf freshens due to anomalous winds, less freshwater actually enters the interior northern Labrador Sea under the same wind regime. We find a negative FWC anomaly off the shelf break in the northern Labrador Sea—the opposite signature of a sea ice melt freshened southeastern shelf (cf. Figures 7d and 7f).

The composite analysis reveals that a direct attribution of FWC anomalies to runoff, sea ice melt and wind stress and their implications for deep convection remains a challenge, because (a) FWC anomalies of different origin or cause have similar magnitudes, (b) years of anomalous runoff may also feature anomalous sea ice melt and/or wind conditions causing a similar freshening, and (c) runoff and sea ice melt peak long before the next deep convection season and varying wind regimes moderate their advection along and export from the boundary current into the interior Labrador and Irminger Seas.

4. Discussion and Conclusions

In this work we use the GLORYS12 reanalysis, an observational-assimilated model-based product, along with the high resolution, eddy-rich ocean model VIKING20X to compare freshwater propagation and variability along the east Greenland shelf and test their potential for identifying imprints of accelerated Greenland ice sheet melt. A mandatory requisite of the data being used for this is a well-resolved EGCC because freshwater is contained on and close to the shelf and surface. We find that the improvement of surface boundary conditions including inter-annually and seasonally varying, local estimates is crucial to realistically simulate the redistribution of meltwater and changes in FWC in the EGCC, which contains the first imprints of Greenland runoff. In line with earlier studies (Castelao et al., 2019; Gillard et al., 2016) we conclude that a sufficiently high spatial resolution should be used to simulate the dynamical interaction between the EGCC and outer EGC and the freshwater pathway along east Greenland and find 1/20° suitable to achieve this.

In the VIKING20X simulation forced with realistic interannually varying runoff, we find two FWC maxima in the EGCC at sections south of major glaciers (Helheim and Kangerlussuaq) in 2010 and 2012 (see Figure 2). During these summers, the Greenland ice sheet experiences extreme melt conditions yielding exceptionally large runoff (Hanna et al., 2014; Slater et al., 2021b; Tedesco et al., 2011). While similarly extreme conditions were observed during 2019 (Sasgen et al., 2020; Slater et al., 2021b), the runoff forcing applied to VIKING20X does include interannual variations in Greenland runoff only until 2016 based on the data from Bamber et al. (2018) and applies the monthly climatology from 2012 to 2016 thereafter (Tsujino et al., 2018) and thus lacks freshening in 2019 comparable to 2010 and 2012. The imprint of strong Greenland meltwater runoff seen in the EGCC is highly dependent on the freshwater forcing. Although local salinity observations are assimilated in GLORYS12, we could not find a comparable imprint in FWC on the east Greenland shelf and conclude that this is due to the runoff forcing applied to GLORYS12 lacking annual estimates of increased Greenland runoff (applying a linear trend instead) and the general lack of in situ observations on the shelf in the upper 50 m, where most of the freshwater is carried with the EGCC. Reanalysis products like GLORYS12 would greatly benefit from intensified Greenland shelf observations and it would be interesting to see whether such observations could compensate a lack in surface boundary conditions detail, such as interannually varying meltwater fluxes. Without such observations, the product relies on the capabilities of the model to simulate shelf processes demanding mesoscale dynamics permitting grid spacing.

Low salinity waters near the shelf are well represented in VIKING20X when compared with mooring data along the OSNAP East array, while GLORYS12 appears more saline close to the shelf (Figure S2 in Supporting Information S1). A significant source of freshwater in the EGC system is determined by Arctic Ocean export. GLORYS12 underestimated FWT through Fram Strait when compared to observations shown in Figure 3, while VIKING20X was comparable to observations. However model biases such as slower current speeds, freshwater export being further confined to the shelf in VIKING20X and higher salinities with freshwater observed at shallower depths in GLORYS12 result in the reduced transport. VIKING20X and GLORYS12 had a mean annual FWF of 44–62 mSv, while observational estimates yield 68 mSv. Since Arctic export is such a significant source of freshwater in the EGC system (Harden et al., 2014) it is crucial to accurately represent high Arctic sources of freshwater and the subsequent export to lower latitudes. Nevertheless, an analysis of freshwater anomalies, such as ours, is likely less affected by biases and variations at and upstream of Fram Strait.

We find that freshwater anomalies are advected from Fram Strait to Cape Farewell within 4–8 months, in agreement with Harden et al. (2014) observing a lag of approximately 4 months between the FWC seasonality at Fram Strait when measured at the mooring array by Sermilik fjord ($\approx 65^\circ\text{N}$). Therefore, late wintertime freshwater anomalies at Fram Strait reach Denmark Strait just at beginning of summer when runoff from Greenland picks up (Figure 4). South of 65°N the Greenland shelf narrows and the boundary current velocity increases, reducing advective time scales to less than 1 month. Particularly in winter where the alongshore northerly winds strengthen, induce onshore transport, and speed up the current.

The overlapping seasonality from freshwater sources highlights the challenge of determining the imprint and impact of enhanced Greenland runoff, given the contribution from freshwater sources such as Arctic Ocean export and regional sea ice melt. Sea ice melt begins during summer at latitudes greater than 68°N , thus occurring at the same time as Greenland runoff is strongest along the coast. However, the VIKING20X simulation shows that south of 65°N , melting of sea ice is largest during late winter and early spring (Figure 5a) contributing to the FWC further downstream at a time well distinguishable from any runoff peak.

The correlation analysis based on Le Bras et al. (2018) shows the role that alongshore surface winds play in the EGCC and outer EGC transport variability. We find a higher correlation at the EGCC than (Le Bras et al., 2018) where the discrepancy may be due to mooring availability close to the shelf. When alongshore winds strengthen and strong onshore Ekman transport steepens the isopycnals speeding up the EGCC, most of the freshwater is constrained within the EGCC. Thus, the FWT variability in the EGCC is more correlated with the changes in wind stress versus the outer EGC. The correlations show that the volume transport variability in the EGCC and outer EGC is consistent with wind-driven mechanisms discussed in previous studies. The FWT correlation, with lower correlation coefficients but still statistically significant, confirmed that the freshest waters are contained within the EGCC close to the shelf whereas the outer EGC is more saline due to lateral mixing from warmer and saltier offshore waters. Most recently, Duyck and de Jong (2023) showed that any exchanges between the south-east Greenland shelf and interior seas, particularly at Cape Farewell, are driven primarily by alongshore winds.

Lastly we investigated the impact on FWC from Greenland runoff, sea ice melt, and alongshore wind stress from composites contrasting exceptionally weak and strong conditions (Figure 7). Increased Greenland runoff and sea ice melt resulted in a fresher boundary current, but the alongshore winds showed that weaker onshore Ekman transport results in a relaxation of the EGCC, where the freshwater constrained to the shelf can widen, laterally increasing the maximum extent beyond the shelf. While the opposite occurs during periods of strong, downwelling-favorable winds where the freshwater is pushed towards the shelf, narrowing the fresh boundary current but allowing saltier water from the interior to mix further with the outer EGC thus resulting in a salinification of the slope and EGCC. After the peak freshwater input from sea ice melt in May, there is a strong FWC anomaly along southeast Greenland which appears to follow the west Greenland current and intrudes into the northern Labrador sea with the anomaly eroding in the interior but results in a freshening of the interior Labrador sea.

In this study, it is evident that disentangling the signals of freshwater contributions by Greenland ice sheet melt, Arctic Ocean export, and sea ice melt still remains a challenge. The potential for enhanced Greenland runoff, longer freshening events in the future, and offshore transport of freshwater could all affect stratification in the interior subpolar gyre. While most of the freshwater from Greenland and the Arctic Ocean stays within the confines of the EGCC and boundary current system after rounding Cape Farewell, its potential to directly enter the deep convection sites in the Labrador Sea depends on the local wind regime and baroclinic instability of the current itself and is subject to strong interannual variability (Castelao et al., 2019; Rieck et al., 2019). The negative mass balance of the Greenland ice sheet has not yet persisted long enough to have a visible impact on the salinity budget and stratification, that is, the FWC, of the SPNA and to affect deep convection (Böning et al., 2016; Devilliers et al., 2021; Dukhovskoy et al., 2019; Luo et al., 2016). However with much more freshwater looming on Greenland (Slater et al., 2021a) or in the Beaufort Gyre of the Arctic Ocean (Proshutinsky et al., 2019; Solomon et al., 2021; Zhang et al., 2021), investigating how freshwater is transported along the EGC system is vital to understand future responses to global warming in the SPNA.

Data Availability Statement

All (processed) model data and scripts needed for Figures 1–7 are made available using the GEOMAR data management platform under the identifier: hdl.handle.net/20.500.12085/fd7a41ce-9cc1-46f9-8ed4-1339880c3c42 (Schiller-Weiss et al., 2023). The CMEMS global ocean physics reanalysis is made available on the Copernicus Marine Service: <https://doi.org/10.48670/moi-00021>. Fram Strait gridded monthly mean velocity and salinity data are available: <https://data.npolar.no/dataset/049178d8-9bd3-42b3-a793-606690a5cd8a>. OSNAP East CTD measurements at Cape Farewell were collected and made freely available by the OSNAP project: www.o-snap.org.

Acknowledgments

This work was supported by the Deutsche Forschungsgemeinschaft (DFG) as project G-Shoex (MA 4039/1-1). The authors wish to thank the Ocean Dynamics working group at GEOMAR. Thank you to Patricia Handmann for fruitful discussions on freshwater in the subpolar North Atlantic, Willi Rath for technical and scientific support, and Klaus Getzlaff for conducting the VIKING20X simulation. Finally, we want to thank the comments of the anonymous reviewers who helped to greatly improve this manuscript. Open Access funding enabled and organized by Projekt DEAL.

References

- Bacon, S., Marshall, A., Holliday, N., Aksenov, Y., & Dye, S. (2014). Seasonal variability of the east Greenland coastal current. *Journal of Geophysical Research: Oceans*, 119(6), 3967–3987. <https://doi.org/10.1002/2013JC009279>
- Bacon, S., Reverfdin, G., Rigor, I., & Snaith, H. (2002). A freshwater jet on the east Greenland shelf. *Journal of Geophysical Research*, 107(C7), 3068. <https://doi.org/10.1029/2001JC000935>
- Bakker, P., Schmittner, A., Lenaerts, J., Abe-Ouchi, A., Bi, D., Van den Broeke, M., et al. (2016). Fate of the Atlantic meridional overturning circulation—Strong decline under continued warming and Greenland melting: AMOC projections for warming & GIS melt. *Geophysical Research Letters*, 43(23), 12252–12260. <https://doi.org/10.1002/2016GL070457>
- Bamber, J., Tedstone, A., King, M., Howat, I., Enderlin, E., Van den Broeke, M., & Noël, B. (2018). Land ice freshwater budget of the arctic and north Atlantic oceans. Part I: Data, methods and results. *Journal of Geophysical Research: Oceans*, 123(3), 1827–1837. <https://doi.org/10.1002/2017JC013605>
- Behrens, E. (2013). The oceanic response to Greenland melting: The effect of increasing model resolution (Unpublished doctoral dissertation). Retrieved from https://macau.uni-kiel.de/receive/diss_mods_00013684
- Belkin, I. M. (2004). Propagation of the “great salinity anomaly” of the 1990s around the northern north Atlantic. *Geophysical Research Letters*, 31(8), L08306. <https://doi.org/10.1029/2003GL019334>
- Biaostoch, A., Schwarzkopf, F., Getzlaff, K., Rühls, S., Martin, T., Scheinert, M., et al. (2021). Regional imprints of changes in the atlantic meridional overturning circulation in the eddy-rich ocean model viking20x. *Ocean Science*, 17(5), 1177–1211. <https://doi.org/10.5194/os-17-1177-2021>
- Böning, C., Behrens, E., Biaostoch, A., Getzlaff, K., & Bamber, J. (2016). Emerging impact of Greenland meltwater on deepwater formation in the North Atlantic Ocean. *Nature Geoscience*, 9(7), 523–527. <https://doi.org/10.1038/ngeo2740>
- Castelao, R., Luo, H., Oliver, H., Rennermalm, A., Tedesco, M., Bracco, A., et al. (2019). Controls on the transport of meltwater from the southern Greenland ice sheet in the Labrador Sea. *Journal of Geophysical Research: Oceans*, 124(6), 3551–3560. <https://doi.org/10.1029/2019JC015159>
- Dai, A., Qian, T., Trenberth, K., & Milliman, J. (2008). Changes in continental freshwater discharge from 1948 to 2004. *Journal of Climate*, 22(10), 2773–2792. <https://doi.org/10.1175/2008JCLI2592.1>

- Debreu, L., Vouland, C., & Blayo, E. (2008). Agrif: Adaptive grid refinement in Fortran. *Computers & Geosciences*, 34(1), 8–13. <https://doi.org/10.1016/j.cageo.2007.01.009>
- de Steur, L., Peralta Ferriz, C., & Pavlova, O. (2018). Freshwater export in the east Greenland current freshens the North Atlantic. *Geophysical Research Letters*, 45(24), 13359–13366. <https://doi.org/10.1029/2018GL080207>
- de Steur, L., Pickart, R., Macrander, A., Våge, K., Harden, B., Jonsson, S., et al. (2016). Liquid freshwater transport estimates from the east Greenland current based on continuous measurements north of Denmark strait. *Journal of Geophysical Research: Oceans*, 122, 93–109. <https://doi.org/10.1002/2016JC012106>
- de Steur, L., Pickart, R., Torres, D., & Valdimarsson, H. (2015). Recent changes in the freshwater composition east of Greenland. *Geophysical Research Letters*, 42(7), 2326–2332. <https://doi.org/10.1002/2014GL062759>
- Devilliers, M., Swingedouw, D., Mignot, J., Deshayes, J., Garric, G., & Ayache, M. (2021). A realistic Greenland ice sheet and surrounding glaciers and ice caps melting in a coupled climate model. *Climate Dynamics*, 57(9–10), 2467–2489. <https://doi.org/10.1007/s00382-021-05816-7>
- Dickson, R., Meincke, J., Malmberg, S.-A., & Lee, A. (1988). The great salinity anomaly in the northern north Atlantic 1968–1982. *Progress in Oceanography*, 20(2), 103–151. [https://doi.org/10.1016/0079-6611\(88\)90049-3](https://doi.org/10.1016/0079-6611(88)90049-3)
- Dickson, R., Rudels, B., Dye, S., Karcher, M., Meincke, J., & Yashayaev, I. (2006). Current estimates of freshwater flux through arctic and subarctic seas. *Progress in Oceanography*, 73(3–4), 210–230. <https://doi.org/10.1016/j.pocan.2006.12.003>
- Drévillon, M., Lellouche, J., Régnier, C., Garric, G., Bricaud, C., & R, H. (2021). Cmems-glo-quid-001-030, 1.4 edn., eu copernicus marine service information [online]. Retrieved from <https://catalogue.marine.copernicus.eu/documents/QUID/CMEMS-GLO-QUID-001-030.pdf>
- Dukhovskoy, D., Myers, P., Platon, G., Timmermans, M.-L., Curry, B., Proshutinsky, A., et al. (2015). Greenland freshwater pathways in the sub-Arctic seas from model experiments with passive tracers. *Journal of Geophysical Research: Oceans*, 121(1), 877–907. <https://doi.org/10.1002/2015JC011290>
- Dukhovskoy, D., Yashayaev, I., Proshutinsky, A., Bamber, J., Bashmachnikov, I., Chassignet, E., et al. (2019). Role of Greenland freshwater anomaly in the recent freshening of the subpolar north Atlantic. *Journal of Geophysical Research: Oceans*, 124(5), 3333–3360. <https://doi.org/10.1029/2018JC014686>
- Duyck, E., & de Jong, M. F. (2023). Cross-shelf exchanges between the east Greenland shelf and interior seas. *Journal of Geophysical Research: Oceans*, 128(7), e2023JC019905. <https://doi.org/10.1029/2023JC019905>
- Duyck, E., Gelderloos, R., & de Jong, M. F. (2022). Wind-driven freshwater export at cape farewell. *Journal of Geophysical Research: Oceans*, 127(5), e2021JC018309. <https://doi.org/10.1029/2021JC018309>
- Fichefet, T., & Morales Maqueda, M. A. (1997). Sensitivity of a global sea ice model to the treatment of ice thermodynamics and dynamics. *Journal of Geophysical Research*, 102(C6), 12609–12646. <https://doi.org/10.1029/97JC00480>
- Fischer, J., Karstensen, J., Oltmanns, M., & Schmidtke, S. (2018). Mean circulation and eke distribution in the Labrador Sea water level of the subpolar north Atlantic. *Ocean Science*, 14(5), 1167–1183. <https://doi.org/10.5194/os-14-1167-2018>
- Foukal, N., Gelderloos, R., & Pickart, R. (2020). A continuous pathway for fresh water along the east Greenland shelf. *Science Advances*, 6(43). <https://doi.org/10.1126/sciadv.abc4254>
- Friedman, A. R., Reverdin, G., Khodri, M., & Gastineau, G. (2017). A new record of Atlantic Sea surface salinity from 1896 to 2013 reveals the signatures of climate variability and long-term trends. *Geophysical Research Letters*, 44(4), 1866–1876. <https://doi.org/10.1002/2017GL072582>
- Frölicher, T., Fischer, E., & Gruber, N. (2018). Marine heatwaves under global warming. *Nature*, 560(7718), 360–364. <https://doi.org/10.1038/s41586-018-0383-9>
- Fuentes-Franco, R., & Koenigk, T. (2019). Sensitivity of the Arctic freshwater content and transport to model resolution. *Climate Dynamics*, 53(3–4), 1765–1781. <https://doi.org/10.1007/s00382-019-04735-y>
- Garcia, C., Comiso, J., Dinnat, E., & Brucker, L. (2017). Satellite observed salinity distributions at high latitudes in the northern hemisphere: A comparison of four products. *Journal of Geophysical Research: Oceans*, 122(9), 7717–7736. <https://doi.org/10.1002/2017JC013184>
- Gascard, J.-C., Richez, C., & Rouault, C. (1995). New insights on large-scale oceanography in Fram Strait: The West Spitsbergen Current. In W. O. Smith & J. M. Grebmeir (Eds.), *Arctic oceanography: Marginal ice zones and continental shelves*. <https://doi.org/10.1029/CE049p0131>
- Gillard, L., Hu, X., Myers, P., & Bamber, J. (2016). Meltwater pathways from marine terminating glaciers of the Greenland ice sheet: Meltwater pathways from the GrIS. *Geophysical Research Letters*, 43(20), 10873–10882. <https://doi.org/10.1002/2016GL070969>
- Good, S., Martin, M., & Rayner, N. (2013). En4: Quality controlled ocean temperature and salinity profiles and monthly objective analyses with uncertainty estimates. *Journal of Geophysical Research: Oceans*, 118(12), 6704–6716. <https://doi.org/10.1002/2013JC009067>
- Guinehut, S., Dhomp, A.-L., Gilles, L., & Traou, P.-Y. (2012). High resolution 3-d temperature and salinity fields derived from in situ and satellite observations. *Ocean Science*, 8(5), 845–857. <https://doi.org/10.5194/os-8-845-2012>
- Haine, T., Curry, B., Gerdes, R., Hansen, E., Karcher, M., Lee, C., et al. (2015). Arctic freshwater export: Status, mechanisms, and prospects. *Global and Planetary Change*, 125, 13–35. <https://doi.org/10.1016/j.gloplacha.2014.11.013>
- Handmann, P. (2019). Deep water formation and spreading dynamics in the subpolar north Atlantic from observations and high-resolution ocean models (Unpublished doctoral dissertation). Retrieved from https://macau.uni-kiel.de/receive/macau_mods_00000258
- Hanna, E., Fettweis, X., Mernild, S., Cappelen, J., Ribergaard, M., Shuman, C., et al. (2014). Atmospheric and oceanic climate forcing of the exceptional Greenland ice sheet surface melt in summer 2012. *International Journal of Climatology*, 34(4), 1022–1037. <https://doi.org/10.1002/joc.3743>
- Hanna, E., Huybrechts, P., Steffen, K., Cappelen, J., Huff, R., Shuman, C., et al. (2008). Increased runoff from melt from the Greenland ice sheet: A response to global warming. *Journal of Climate*, 21(2), 331–341. <https://doi.org/10.1175/2007JCLI1964.1>
- Harden, B., Straneo, F., & Sutherland, D. (2014). Moored observations of synoptic and seasonal variability in the east Greenland coastal current. *Journal of Geophysical Research: Oceans*, 119(12), 8838–8857. <https://doi.org/10.1002/2014JC010134>
- Håvik, L., Pickart, R., Våge, K., Torres, D., Thurnherr, A., Beszczynska-Moeller, A., et al. (2017). Evolution of the east Greenland current from fram strait to Denmark strait: Synoptic measurements from summer 2012. *Journal of Geophysical Research: Oceans*, 122(3), 1974–1994. <https://doi.org/10.1002/2016JC012228>
- Håvik, L., & Våge, K. (2018). Wind-driven coastal upwelling and downwelling in the shelfbreak east Greenland current. *Journal of Geophysical Research: Oceans*, 123(9), 6106–6115. <https://doi.org/10.1029/2018JC014273>
- Hobday, A., Oliver, E., Gupta, A., Benthuyzen, J., Burrows, M., Donat, M., et al. (2018). Categorizing and naming marine heatwaves. *Oceanography*, 31(2). <https://doi.org/10.5670/oceanog.2018.205>
- Holford, J., & Hansen, E. (2005). Timeseries of polar water properties in fram strait. *Geophysical Research Letters*, 32(19), L19601. <https://doi.org/10.1029/2005GL022957>
- Holliday, N., Bersch, M., Bex, B., Chafik, L., Cunningham, S., Florindo-López, C., et al. (2020). Ocean circulation causes the largest freshening event for 120 years in eastern subpolar north Atlantic. *Nature Communications*, 11(1), 585. <https://doi.org/10.1038/s41467-020-14474-y>

- Holliday, N., Meyer, A., Bacon, S., Alderson, S., & Cuevas, B. (2007). Retroflexion of part of the east Greenland current at cape farewell. *Geophysical Research Letters*, 34(7), L07609. <https://doi.org/10.1029/2006GL029085>
- Jackson, L., & Wood, R. (2018). Timescales of AMOC decline in response to fresh water forcing. *Climate Dynamics*, 51(4), 1333–1350. <https://doi.org/10.1007/s00382-017-3957-6>
- Karpouzoglou, T., de Steur, L., Smedsrud, L., & Sumata, H. (2022). Observed changes in the Arctic freshwater outflow in fram strait. *Journal of Geophysical Research: Oceans*, 127(3), e2021JC018122. <https://doi.org/10.1029/2021JC018122>
- Koehler, J., Sena-Martins, M., Serra, N., & Stammer, D. (2014). Quality assessment of spaceborne sea surface salinity observations over the northern north Atlantic. *Journal of Geophysical Research: Oceans*, 120(6), 4306–4323. <https://doi.org/10.1002/2014JC010067>
- Le Bras, I., Straneo, F., Holte, J., & Holliday, N. (2018). Seasonality of freshwater in the east Greenland current system from 2014 to 2016. *Journal of Geophysical Research: Oceans*, 123(12), 8828–8848. <https://doi.org/10.1029/2018JC014511>
- Lellouche, J.-M., Greiner, E., Bourdallé-Badie, R., Garric, G., Melet, A., Drevillon, M., et al. (2021). The copernicus global 1/12° oceanic and sea ice GLORYS12 reanalysis. *Frontiers in Earth Science*, 9, 698876. <https://doi.org/10.3389/feart.2021.698876>
- Locarnini, R. A., Mishonov, A. V., Antonov, J. I., Boyer, T. P., Garcia, H. E., Baranova, O. K., et al. (2013). In S. Levitus (Ed.), A. Mishonov (Technical Ed.), *World Ocean Atlas 2013 volume 1: Temperature*. NOAA Atlas NESDIS 73 (40 pp.). <https://doi.org/10.7289/V55X26VD>
- Lozier, M., Li, F., Bacon, S., Bahr, F., Bower, A., Cunningham, S., et al. (2019). A sea change in our view of overturning in the subpolar north Atlantic. *Science*, 363(6426), 516–521. <https://doi.org/10.1126/science.aau6592>
- Luo, H., Castelao, R., Rennermalm, A., Tedesco, M., Bracco, A., Yager, P., & Mote, T. (2016). Oceanic transport of surface meltwater from the southern Greenland ice sheet. *Nature Geoscience*, 9(7), 528–532. <https://doi.org/10.1038/ngeo2708>
- Madec, G., Bourdallé-Badie, R., Bouttier, P. A., Bricaud, C., Bruciaferri, D., Calvert, D., & Vancoppenolle, M. (2016). Nemo ocean engine. *Scientific notes of climate modeling center* (27). Institut Pierre Simon Laplace (IPSL). <https://doi.org/10.5281/zenodo.8167700>
- Marshall, J., Scott, J., & Proshutinsky, A. (2017). Climate response functions for the Arctic Ocean: A proposed coordinated modelling experiment. *Geoscientific Model Development*, 10(7), 2833–2848. <https://doi.org/10.5194/gmd-10-2833-2017>
- Martin, T., & Biastoch, A. (2023). On the ocean's response to enhanced Greenland runoff in model experiments: Relevance of mesoscale dynamics and atmospheric coupling. *Ocean Science*, 19(1), 141–167. <https://doi.org/10.5194/os-19-141-2023>
- Moore, G. (2012). A new look at Greenland flow distortion and its impact on barrier flow, tip jets and coastal oceanography. *Geophysical Research Letters*, 39(22), L22806. <https://doi.org/10.1029/2012gl054017>
- Moore, G. (2014). In *A new look at Southeast Greenland barrier winds and katabatic flow* (Vol. 12). US CLIVAR Variations News1.
- Mulet, S., Rio, M.-H., Mignot, A., Guinehut, S., & Morrow, R. (2012). A new estimate of the global 3d geostrophic ocean circulation based on satellite data and in-situ measurements. *Deep Sea Research Part II: Topical Studies in Oceanography*, 77–80, 70–81. <https://doi.org/10.1016/j.dsr2.2012.04.012>
- Myers, P., Donnelly, C., & Ribergaard, M. (2009). Structure and variability of the west Greenland current in summer derived from 6 repeat standard sections. *Progress in Oceanography*, 80(1–2), 93–112. <https://doi.org/10.1016/j.pcean.2008.12.003>
- Olmedo, E., Gabarro, C., González-Gambau, V., Martínez, J., Ballabrera, J., Turiel, A., et al. (2018). Seven years of SMOS sea surface salinity at high latitudes: Variability in arctic and sub-arctic regions. *Remote Sensing*, 10(11), 1772. <https://doi.org/10.3390/rs10111772>
- Oltmanns, M., Karstensen, J., & Fischer, J. (2018). Increased risk of a shutdown of ocean convection posed by warm north Atlantic summers. *Nature Climate Change*, 8(4), 300–304. <https://doi.org/10.1038/s41558-018-0105-1>
- Perkins-Kirkpatrick, S., & Alexander, L. (2013). On the measurement of heat waves. *Journal of Climate*, 26(13), 4500–4517. <https://doi.org/10.1175/JCLI-D-12-00383.1>
- Proshutinsky, A., Krishfield, R., Toole, J., Timmermans, M., Williams, W., Zimmerman, S., et al. (2019). Analysis of the beaufort gyre freshwater content in 2003–2018. *Journal of Geophysical Research: Oceans*, 124(12), 9658–9689. <https://doi.org/10.1029/2019JC015281>
- Rahmstorf, S., Box, J., Feulner, G., Mann, M., Robinson, A., Rutherford, S., & Schaffernicht, E. (2015). Exceptional twentieth-century slowdown in Atlantic ocean overturning circulation. *Nature Climate Change*, 5, 475–480. <https://doi.org/10.1038/nclimate2554>
- Richter, M., von Appen, W.-J., & Wekerle, C. (2018). Does the east Greenland current exist in the northern fram strait? *Ocean Science*, 14(5), 1147–1165. <https://doi.org/10.5194/os-14-1147-2018>
- Rieck, J., Böning, C., & Getzlaff, K. (2019). The nature of eddy kinetic energy in the Labrador Sea: Different types of mesoscale eddies, their temporal variability, and impact on deep convection. *Journal of Physical Oceanography*, 49(8), 2075–2094. <https://doi.org/10.1175/jpo-d-18-0243.1>
- Rignot, E., & Mouginot, J. (2012). Ice flow in Greenland for the international polar year 2008–2009. *Geophysical Research Letters*, 39(11), L11501. <https://doi.org/10.1029/2012GL051634>
- Rignot, E., Velicogna, I., Van den Broeke, M., Monaghan, A., & Lenaerts, J. (2011). Acceleration of the contribution of the Greenland and Antarctic ice sheets to sea level rise. *Geophysical Research Letters*, 38(5), L05503. <https://doi.org/10.1029/2011GL046583>
- Rudels, B., Jones, E., Schauer, U., & Eriksson, P. (2004). Atlantic sources of the Arctic Ocean surface and halocline waters. *Polar Research*, 23(2), 181–208. <https://doi.org/10.1111/j.1751-8369.2004.tb00007.x>
- Rühs, S., Oliver, E., Biastoch, A., Böning, C., Dowd, M., Getzlaff, K., et al. (2021). Changing spatial patterns of deep convection in the subpolar north Atlantic. *Journal of Geophysical Research: Oceans*, 126(7). <https://doi.org/10.1029/2021JC017245>
- Sasgen, I., Wouters, B., Gardner, A., King, M., Tedesco, M., Landerer, F., et al. (2020). Return to rapid ice loss in Greenland and record loss in 2019 detected by the grace-fo satellites. *Communications Earth & Environment*, 1, 8. <https://doi.org/10.1038/s43247-020-0010-1>
- Schiller-Weiss, I., Martin, T., Karstensen, J., & Biastoch, A. (2023). Supplementary material to: Do salinity variations along the east Greenland shelf show imprints of increasing meltwater runoff? [Dataset]. GEOMAR Helmholtz Centre for Ocean Research Kiel [distributor]. <https://hdl.handle.net/20.500.12085/fd7a41ce-9cc1-46f9-8ed4-1339880c3c42>
- Slater, T., Lawrence, I., Otsuka, I., Shepherd, A., Gourmelen, N., Jakob, L., et al. (2021a). Review article: Earth's ice imbalance. *The Cryosphere*, 15(1), 233–246. <https://doi.org/10.5194/tc-15-233-2021>
- Slater, T., Shepherd, A., McMillan, M., Leeson, A., Gilbert, L., Muir, A., et al. (2021b). Increased variability in Greenland ice sheet runoff from satellite observations. *Nature Communications*, 12(1), 6069. <https://doi.org/10.1038/s41467-021-26229-4>
- Smedsrud, L., Sorteberg, A., & Kloster, K. (2008). Recent and future changes of the arctic sea-ice cover. *Geophysical Research Letters*, 35(20), L20503. <https://doi.org/10.1029/2008GL034813>
- Solomon, A., Heuzé, C., Rabe, B., Bacon, S., Bertino, L., Heimbach, P., et al. (2021). Freshwater in the Arctic Ocean 2010–2019. *Ocean Science*, 17(4), 1081–1102. <https://doi.org/10.5194/os-17-1081-2021>
- Spreen, G., de Steur, L., Divine, D., Gerland, S., Hansen, E., & Kwok, R. (2020). Arctic sea ice volume export through fram strait from 1992 to 2014. *Journal of Geophysical Research: Oceans*, 125(6), e2019JC016039. <https://doi.org/10.1029/2019JC016039>
- Sutherland, D., & Pickart, R. (2008). The east Greenland coastal current: Structure, variability, and forcing. *Progress in Oceanography*, 78(1), 58–77. <https://doi.org/10.1016/j.pcean.2007.09.006>

- Swingedouw, D., Houssais, M.-N., Herbaut, C., Blaizot, A.-C., Devilliers, M., & Deshayes, J. (2022). AMOC recent and future trends: A crucial role for oceanic resolution and Greenland melting? *Frontiers in Climate*, 4. <https://doi.org/10.3389/fclim.2022.838310>
- Swingedouw, D., Rodehacke, C., Behrens, E., Menary, M., Olsen, S., Gao, Y., et al. (2012). Decadal fingerprints of freshwater discharge around Greenland in a multi-model ensemble. *Climate Dynamics*, 41(3–4), 695–720. <https://doi.org/10.1007/s00382-012-1479-9>
- Tedesco, M., Fettweis, X., Van den Broeke, M., Wal, R., Smeets, P., Berg, W., et al. (2011). The role of albedo and accumulation in the 2010 melting record in Greenland. *Environmental Research Letters*, 6(1), 014005. <https://doi.org/10.1088/1748-9326/6/1/014005>
- Tesdal, J.-E., Abernathey, R., Goes, J., Gordon, A., & Haine, T. (2018). Salinity trends within the upper layers of the subpolar north Atlantic. *Journal of Climate*, 31(7), 2675–2698. <https://doi.org/10.1175/JCLI-D-17-0532.1>
- Tournadre, J., Bouhier, N., Girard-Ardhuin, F., & Rémy, F. (2015). Antarctic icebergs distributions 1992–2014. *Journal of Geophysical Research: Oceans*, 121(1), 327–349. <https://doi.org/10.1002/2015JC011178>
- Tsujino, H., Urakawa, S., Nakano, H., Small, R., Kim, W., Yeager, S., et al. (2018). Jra-55 based surface dataset for driving ocean—Sea-ice models (jra55-do). *Ocean Modelling*, 130, 79–139. <https://doi.org/10.1016/j.ocemod.2018.07.002>
- Våge, K., Papritz, L., Håvik, L., Spall, M., & Moore, G. (2018). Ocean convection linked to the recent ice edge retreat along east Greenland. *Nature Communications*, 9(1), 1287. <https://doi.org/10.1038/s41467-018-03468-6>
- Vinje, T. (2001). Fram strait ice fluxes and atmospheric circulation: 1950–2000. *Journal of Climate*, 14(16), 3508–3517. [https://doi.org/10.1175/1520-0442\(2001\)014<3508:FSIFAA>2.0.CO;2](https://doi.org/10.1175/1520-0442(2001)014<3508:FSIFAA>2.0.CO;2)
- Wang, Q., Ricker, R., & Mu, L. (2021). Arctic sea ice decline preconditions events of anomalously low sea ice volume export through fram strait in the early 21st century. *Journal of Geophysical Research: Oceans*, 126(2), e2020JC016607. <https://doi.org/10.1029/2020JC016607>
- Zhang, J., Weijer, W., Steele, M., Cheng, W., Verma, T., & Veneziani, M. (2021). Labrador sea freshening linked to beaufort gyre freshwater release. *Nature Communications*, 12(1), 1229. <https://doi.org/10.1038/s41467-021-21470-3>
- Zou, S., Lozier, M., Li, F., Abernathey, R., & Jackson, L. (2020). Density-compensated overturning in the Labrador sea. *Nature Geoscience*, 13(2), 1–6. <https://doi.org/10.1038/s41561-019-0517-1>
- Zweng, M. M., Reagan, J. R., Antonov, J. I., Locarnini, R. A., Mishonov, A. V., Boyer, T. P., et al. (2013). In S. Levitus (Ed.), A. Mishonov (Technical Ed.), *World Ocean Atlas 2013 volume 2: Salinity*. NOAA Atlas NESDIS 74 (39 pp.). <https://doi.org/10.7289/V5251G4D>